Lipocalin 2-Dependent Inhibition of Mycobacterial Growth in Alveolar Epithelium[1]

Hiroyuki Saiga,*† Junichi Nishimura,* Hirotaka Kuwata,† Megumi Okuyama,* Sohkichi Matsumoto,‖ Shintaro Sato,§ Makoto Matsumoto,† Shizuo Akira,§¶ Yasunobu Yoshikai,‡ Kenya Honda,* Masahiro Yamamoto,* and Kiyoshi Takeda[2]*†¶

Mycobacterium tuberculosis invades alveolar epithelial cells as well as macrophages. However, the role of alveolar epithelial cells in the host defense against *M. tuberculosis* remains unknown. In this study, we report that lipocalin 2 (Lcn2)-dependent inhibition of mycobacterial growth within epithelial cells is required for anti-mycobacterial innate immune responses. Lcn2 is secreted into the alveolar space by alveolar macrophages and epithelial cells during the early phase of respiratory mycobacterial infection. Lcn2 inhibits the in vitro growth of mycobacteria through sequestration of iron uptake. Lcn2-deficient mice are highly susceptible to intratracheal infection with *M. tuberculosis*. Histological analyses at the early phase of mycobacterial infection in Lcn2-deficient mice reveal increased numbers of mycobacteria in epithelial cell layers, but not in macrophages, in the lungs. Increased intracellular mycobacterial growth is observed in alveolar epithelial cells, but not in alveolar macrophages, from Lcn2-deficient mice. The inhibitory action of Lcn2 is blocked by the addition of endocytosis inhibitors, suggesting that internalization of Lcn2 into the epithelial cells is a prerequisite for the inhibition of intracellular mycobacterial growth. Taken together, these findings highlight a pivotal role for alveolar epithelial cells during mycobacterial infection, in which Lcn2 mediates anti-mycobacterial innate immune responses within the epithelial cells. *The Journal of Immunology*, 2008, 181: 8521–8527.

Tuberculosis is a worldwide disease caused by infection with *Mycobacterium tuberculosis*. Therefore, the host defense mechanisms against *M. tuberculosis* have been intensively investigated, and important roles of T cell-mediated adaptive immunity have been well established (1, 2). In addition, functional characterization of TLRs has recently indicated the importance of innate immunity in the host responses to infection with *M. tuberculosis* (3, 4). In the TLR-mediated anti-mycobacterial immune responses, macrophages and dendritic cells are major effectors that engulf pathogens and produce a variety of proinflammatory mediators. In respiratory mycobacterial infection, alveolar macrophages are the major targets of invasion. However, several evidences indicate that mycobacteria also interact with epithelial cells in the respiratory tract and invade these cells (5–9). Accordingly, epithelial cells in the lungs are expected to play a role during mycobacterial infection by producing antimicrobial mediators (10).

Lipocalin 2 (Lcn2),[3] also known as neutrophil gelatinase-associated lipocalin, siderocalin, 24p3, or uterocalin, a member of the lipocalin family of proteins that bind to small hydrophobic molecules, is produced by epithelial cells and macrophages (11–16). Lcn2 has been shown to mediate several biological processes, including mammary gland involution, induction of apoptosis, and delivery of iron (12, 17–19). In addition, structural studies have demonstrated that Lcn2 binds to enterobactin-type bacterial siderophores, which facilitate iron uptake by bacteria (16). Subsequent studies revealed that Lcn2 also binds to other types of siderophores, such as carboxy-mycobactin (produced by mycobacteria) and bacillibactin (produced by *Bacillus anthracis*) (20, 21). Lcn2 has been shown to interfere with siderophore-mediated iron uptake in *Escherichia coli* (16). Accordingly, mice deficient in Lcn2 are highly susceptible to infection with *E. coli* (22, 23). Thus, Lcn2 mediates the host defense against *E. coli* infection through sequestration of iron, which is essential for the growth and activity of nearly all bacteria (24).

Mycobacteria replicate within cells, especially in the phagosome of macrophages (25), where iron is limited. Outside host cells, free iron is also limited, because almost all iron ions exist as complexes with host proteins with high affinity for iron, such as transferrin and lactoferrin. To overcome the iron deficiency within the host, some species of mycobacteria, such as *M. tuberculosis* and *Mycobacterium bovis* bacillus Calmette-Guérin (BCG), synthesize two type of siderophores, called mycobactin and carboxy-mycobactin (also called exochelin) (26, 27). Mycobactin is hydrophobic, whereas carboxy-mycobactin is hydrophilic. These mycobactins have been shown to remove iron from host iron-binding proteins, such as transferrin and lactoferrin (28). In addition, *M. tuberculosis*

*Laboratory of Immune Regulation, Department of Microbiology and Immunology, Graduate School of Medicine, Osaka University, Suita, Osaka, Japan; †Department of Molecular Genetics and ‡Division of Host Defense, Research Center for Prevention of Infectious Diseases, Medical Institute of Bioregulation, Kyushu University, Fukuoka, Japan; §Department of Host Defense, Research Institute for Microbial Diseases and ¶WPI Immunology Frontier Research Center, Osaka University, Suita, Osaka, Japan; and ‖Department of Bacteriology, Osaka City University Graduate School of Medicine, Osaka, Japan

Received for publication August 5, 2008. Accepted for publication October 11, 2008.

The costs of publication of this article were defrayed in part by the payment of page charges. This article must therefore be hereby marked *advertisement* in accordance with 18 U.S.C. Section 1734 solely to indicate this fact.

[1] This work was supported by a Grant-in-Aid from the Ministry of Education, Culture, Sports, Science and Technology and the Ministry of Health, Labor and Welfare, as well as the Osaka Foundation for the Promotion of Clinical Immunology.

[2] Address correspondence and reprint requests to Dr. Kiyoshi Takeda, Laboratory of Immune Regulation, Department of Microbiology and Immunology, Graduate School of Medicine, Osaka University, Suita, Osaka, Japan. E-mail address: ktakeda@ongene.med.osaka-u.ac.jp

[3] Abbreviations used in this paper: Lcn2, lipocalin 2; BCG, *Mycobacterium bovis* bacillus Calmette-Guérin; BALF, bronchoalveolar lavage fluid; rLcn2, recombinant Lcn2; SP-C, pro-surfactant protein C; DFO, deferoxamine; AEC, alveolar epithelial cell; CPZ, chlorpromazine.

with mutations in the *mbtB* gene, which lack carboxy-mycobactin and mycobactin, exhibit impaired replication in low-iron medium and within macrophages (27). The mechanisms for the mycobactin-mediated iron acquisition within the phagosome of macrophages have recently been elucidated (29). Because pulmonary epithelial cells are also invaded by mycobacteria, host defense mechanisms that inhibit mycobacterial replication within these cells are expected to exist, however they currently remain unclear.

In the present study, we analyzed the role of Lcn2 in mycobacterial infection. Lcn2, which inhibits mycobacterial growth, was rapidly produced from alveolar macrophages and epithelial cells after mycobacterial infection. Furthermore, analyses using Lcn2-deficient mice revealed a pivotal role of alveolar epithelial cells in mycobacterial infection.

Materials and Methods

Mice

Lcn2$^{-/-}$ and *H-2K*^{b}*-tsA58* transgenic mice have been generated (22, 30) and backcrossed to C57BL/6 for six generations. *Lcn2*$^{-/-}$ and wild-type littermates from intercrosses of *Lcn2*$^{+/-}$ mice were used for experiments at 6–8 wk of age. All animal experiments were conducted in accordance with the guidelines of the Animal Care and Use Committee of Kyushu University and Osaka University.

Mycobacteria

M. bovis BCG (Tokyo strain) was purchased from Kyowa Pharmaceuticals. *M. tuberculosis* strains H37Ra (ATCC25177) and H37Rv (ATCC358121) were grown in Middlebrook 7H9-ADC medium for 2 wk and stored at −80°C until use. GFP-expressing BCG, which was generated previously (5), was used for the experiment.

Quantitative real-time RT-PCR

Total RNA was isolated with the TRIzol reagent (Invitrogen), and reverse transcribed using M-MLV reverse transcriptase (Promega) and random primers (Toyobo) after treatment with RQ1 DNaseI (Promega). Quantitative real-time PCR was performed in ABI7300 (Applied Biosystems) using TaqMan Universal PCR Master Mix (Applied Biosystems). All data are shown as the relative mRNA levels normalized by the corresponding 18S rRNA level. The primers for 18S rRNA and Lcn2 were purchased from Assays on Demand (Applied Biosystems).

Preparation of alveolar macrophages

Bronchoalveolar lavage fluid (BALF) was collected from uninfected mice. To eliminate contamination by bacteria, the cells were cultured with 50 U/ml penicillin and 50 μg/ml streptomycin for 16 h, and then washed five times to remove nonadherent cells. The resultant adherent cells were used for experiments as alveolar macrophages, because >95% of the adherent cells were CD11b-positive.

Preparation of recombinant Lcn2 (rLcn2) protein

A mouse Lcn2 cDNA fragment was inserted into pGEX6P-2 (GE Healthcare) and transformed into *E. coli* BL21. The expressed GST-Lcn2 fusion proteins were purified using glutathione-Sepharose 4B (GE Healthcare) according to the manufacturer's instructions. The purified proteins were incubated with PreScission Protease (GE Healthcare) to cleave the GST tag, and then purified with Glutathione-Sepharose 4B.

Immunohistochemistry

Lungs were fixed with 4% PFA and frozen in Tissue-Tec OCT compound (Sakura). The sections were incubated with anti-mouse Lcn2 Ab (R&D Systems), anti-pro-surfactant protein C (SP-C) Ab (Chemicon), anti-CD11b Ab (BD Biosciences), or anti-pan cytokeratin Ab (Sigma-Aldrich). The nuclei were stained with 4′,6-diamidino-2-phenylindole (DAPI; Molecular Probes). Alveolar epithelial cells were infected with GFP-expressing BCG for 16 h, washed, and incubated with Dextran Conjugates (Cascade Blue; Molecular Probes) and Alexa Fluor 594-labeled rLcn2 for 6 h. rLcn2 was labeled using an Alexa Fluor 594 Protein Labeling Kit (Molecular Probes). The cells were fixed with 4% PFA and analyzed using a confocal microscopy (LSM 510; Carl Zeiss).

Western blot assay

BALF was collected from BCG-infected mice by catheterization techniques into 500 μl of PBS. To normalize BALF samples, we injected the same volume of PBS (500 μl), recovered equal volume, and used them for Western blot analysis. After removal of precipitates, the samples were separated on SDS-PAGE and transferred to PVDF membranes (Millipore). The membranes were incubated with anti-mouse Lcn2 Ab. Bound Ab was detected with SuperSignal West Pico Chemiluminescent Substrate (Pierce).

In vitro mycobacterial growth assay

Mycobacteria were incubated in Middlebrook 7H9-ADC medium with the indicated concentrations of rLcn2 protein for 20 days at 37°C, and were plated on Middlebrook 7H10-OADC agar plates and incubated at 37°C for 30 days. In some experiments, BCG was incubated with the indicated concentrations of deferoxamine mesylate (DFO; Calbiochem), $FeCl_3$, or mycobactin (Kyoritsu Seiyaku) on 7H10-OADC agar plates.

In vivo infection of mycobacteria

Mice were intratracheally infected with *M. tuberculosis* H37Rv (1×10^6 CFU). At 6 wk after infection, homogenates of the lungs and livers were plated on 7H10-OADC agar plates. For histological analyses, the lungs were fixed with 4% PFA at 20 or 5 days after infection, embedded in paraffin, cut into sections, and stained with H&E or by the Ziehl-Neelsen method, respectively.

Establishment of alveolar epithelial cell lines

To establish alveolar epithelial cell lines (AECs) from wild-type and *Lcn2*$^{-/-}$ mice, the mice were crossed with *H-2K*^{b}*-tsA58* transgenic mice, and used for experiments at 4 wk of age. Mouse pulmonary type II AECs were established as previously described (32). The cells were incubated at 33°C and passaged over ten times. The cells were then stained with anti-SP-C Ab to confirm that they were type II alveolar epithelial cells.

In vitro infection of mycobacteria

Wild-type or *Lcn2*$^{-/-}$ derived AECs or alveolar macrophages were incubated with BCG for the indicated periods. To eliminate extracellular BCG, the cells were cultured with 50 μg/ml streptomycin for 1 h, washed three times, and harvested. Lysates of the cells were plated on 7H10-OADC agar plates.

Detection of intracellular growth of mycobacteria

Wild-type and *Lcn2*$^{-/-}$-derived AECs were seeded onto 96-well plates, and infected with BCG for 6 h. To eliminate extracellular BCG, the AECs were cultured with 50 μg/ml streptomycin for 1 h, vigorously washed three times. The cells were pulsed with 37 kBq of [^{3}H]uracil and cultured for 48 h. The cells were harvested on glass fiber filters and the incorporated [^{3}H]uracil was measured using a liquid scintillation counter (Wallac). In some experiments, cytochalasin B (Sigma-Aldrich) or chlorpromazine (CPZ; Calbiochem) was added to the wells at 30 min before the [^{3}H]uracil pulse or rLcn2 addition.

Statistical analysis

Differences between control and experimental groups were evaluated using Student's *t* test or ANOVA plus posthoc testing. Values of $p < 0.05$ were considered to indicate statistical significance.

Results

Expression of lipocalin 2 in BCG-infected lungs

To assess the role of Lcn2 in mycobacterial infection, we first analyzed the expression of Lcn2 in the lungs of C57BL/6 mice intratracheally infected with BCG. Total RNA was extracted from the lungs at 2, 7, and 14 days after infection, and analyzed for Lcn2 mRNA expression by real-time quantitative PCR (Fig. 1*A*). Expression of Lcn2 mRNA was markedly increased at 2 days after infection and decreased thereafter. Because Lcn2 mRNA expression was shown to be induced in macrophages stimulated with TLR ligands (22), we analyzed whether alveolar macrophages expressed Lcn2 mRNA (Fig. 1*B*). Alveolar macrophages were isolated, infected with BCG, and analyzed for Lcn2 mRNA expression at 2 days

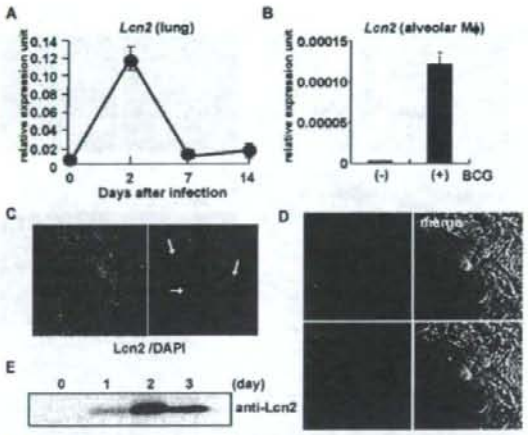

FIGURE 1. Lcn2 expression in the lungs of BCG-infected mice. *A*, Wild-type C57BL/6 mice were intratracheally infected with 2.5×10^6 CFU of BCG. Total RNA was extracted from the lungs after the indicated periods. Lcn2 mRNA expression was analyzed by real-time quantitative PCR. Data are shown as the relative mRNA levels normalized by the corresponding 18S rRNA level. Data are presented as means ± SD, and are representative of two independent experiments. *B*, Alveolar macrophages were isolated from uninfected wild-type mice, cultured with or without BCG for 48 h, and then analyzed for their Lcn2 mRNA expression by real-time quantitative PCR. *C* and *D*, At 2 days after intratracheal infection with BCG, lung tissue sections were stained with anti-Lcn2 Ab (red), DAPI (blue), and anti-SP-C Ab (green), and visualized by fluorescence microscopy. *E*, Wild-type mice were intratracheally infected with 2.5×10^6 CFU of BCG. At the indicated time points after the infection, 500 μl of PBS was intratracheally injected and then recovered. The recovered BALF samples were subjected to Western blot analysis with anti-Lcn2 Ab.

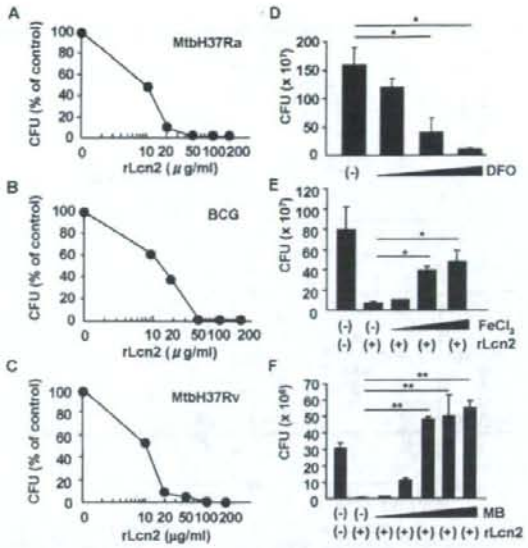

FIGURE 2. Inhibition of in vitro mycobacterial growth by Lcn2. *A–C*, *M. tuberculosis* H37Ra (*A*), BCG (*B*), or *M. tuberculosis* H37Rv (*C*) (1×10^6 CFU each) was incubated with the indicated concentrations of rLcn2 in 7H9 ADC medium for 20 days and then plated on 7H10-OADC agar. The CFU numbers were counted. *D*, BCG was incubated with increasing concentrations of DFO (1 μM, 100 μM and 1 mM) for 20 days and then plated on 7H10-OADC agar. The CFU numbers were counted. *E* and *F*, BCG was incubated in the presence of rLcn2 (50 μg/ml) as well as increasing concentrations of $FeCl_3$ (*E*: 5 nM, 500 nM, 50 μM, and 5 mM) or MB (*F*: 1 pg/ml, 10 pg/ml, 1 ng/ml, 100 ng/ml, and 10 μg/ml) (*F*) for 20 days, and then plated on 7H10-OADC agar. All data are presented as means ± SD. * and ** indicate a significant difference among groups, ANOVA, posthoc Scheffe; *, $p < 0.05$; **, $p < 0.005$.

after infection; BCG infection led to a marked increase in the expression of Lcn2 mRNA. We also analyzed the lungs by immunohistochemistry using an anti BCG-infected mice, several Lcn2-positive cells were observed. These cells mainly faced the alveolar surface and projected into the alveolar space, representing the typical morphology of type II alveolar epithelial cells. Costaining with an Ab to pro-SP-C, which is produced by type II alveolar epithelial cells, revealed that both Lcn2 and SP-C were produced by the same cells (Fig. 1*D*). These findings indicate that not only alveolar macrophages but also type II alveolar epithelial cells produce Lcn2 during respiratory mycobacterial infection. Type II alveolar epithelial cells are known to secrete several mediators into the alveolar space. Therefore, we analyzed whether Lcn2 is secreted into the alveolar space during intratracheal BCG infection. BALF was collected from uninfected and BCG-infected mice and analyzed for Lcn2 protein expression by Western blotting (Fig. 1*E*). Lcn2 was not detected in BALF from uninfected mice. At 2 days after BCG infection, Lcn2 expression was abundantly detected in BALF from the infected mice, indicating that Lcn2 was secreted into the alveolar space during the early phase of mycobacterial infection.

Lcn2-mediated inhibition of mycobacterial growth

We produced rLcn2 and analyzed its effect on in vitro mycobacterial growth. Addition of rLcn2 dose-dependently inhibited the growth of avirulent strains of mycobacteria such as BCG and *M. tuberculosis* H37Ra (Fig. 2, *A* and *B*). rLcn2 also inhibited the growth of virulent *M. tuberculosis* H37Rv in a dose-dependent manner (Fig. 2*C*). Thus, Lcn2 has the ability to inhibit the growth of several mycobacterial strains.

We investigated whether Lcn2 inhibits mycobacterial growth by interfering with iron acquisition, similar to the case for inhibition of *E. coli* growth (16). First, we added DFO, an iron chelator, into in vitro BCG cultures (Fig. 2*D*). DFO reduced BCG growth in a dose-dependent manner, indicating that BCG requires iron for growth. Next, we added ferric iron into BCG cultures (Fig. 2*E*). Addition of ferric iron rescued Lcn2-mediated inhibition of BCG growth in a dose-dependent manner, indicating that Lcn2 inhibits use of iron from the culture medium. Addition of exogenous mycobactin (MB) also abolished Lcn2-mediated inhibition of BCG growth (Fig. 2*F*). These findings indicate that Lcn2 inhibits mycobacterial growth by sequestering iron.

In vivo anti-mycobacterial activity of lipocalin 2

We next addressed the in vivo role of Lcn2 in *M. tuberculosis* infection using *Lcn2*$^{-/-}$ mice. Wild-type and *Lcn2*$^{-/-}$ mice were intratracheally infected with *M. tuberculosis* H37Rv and monitored for their survival (Fig. 3*A*). *Lcn2*$^{-/-}$ mice were highly sensitive to intratracheal infection with *M. tuberculosis* and many of the infected mice died. We also counted the CFU numbers in the lungs and livers after 6 wk of infection (Fig. 3*B*). The CFU titer of *M. tuberculosis* was higher in *Lcn2*$^{-/-}$ mice than that in wild-type mice. Histopathological analysis of the lungs of the infected mice at 20 days after infection revealed that the number and size of the granulomatous lesions were increased in *Lcn2*$^{-/-}$ mice (Fig. 3*C*), indicating that the inflammatory response in *Lcn2*$^{-/-}$ mice was enhanced, possibly due to progression of the *M. tuberculosis* infection. These findings demonstrate that Lcn2 plays an important role in host resistance to *M. tuberculosis* infection in vivo.

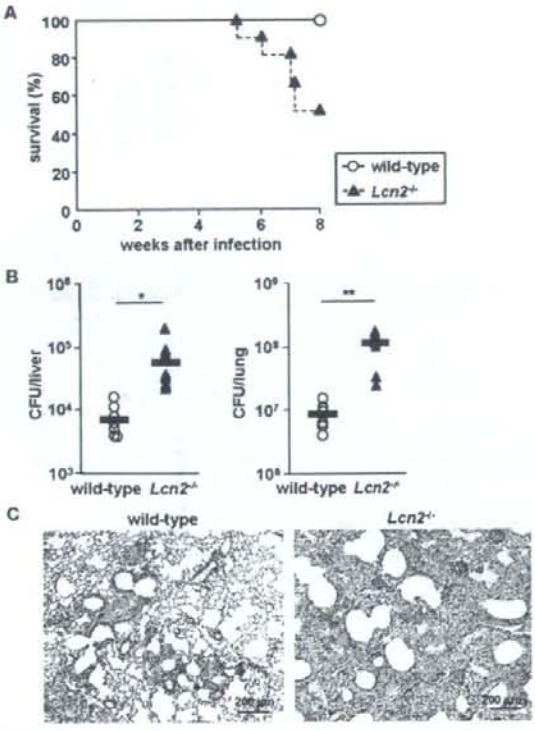

FIGURE 3. High susceptibility of *Lcn2*$^{-/-}$ mice to *M. tuberculosis* infection. *A*, Wild-type ($n = 11$) and *Lcn2*$^{-/-}$ ($n = 12$) mice were intratracheally infected with *M. tuberculosis* H37Rv (1×10^6 CFU) and their survival was monitored for 8 wk. *B*, Wild-type ($n = 7$) and *Lcn2*$^{-/-}$ ($n = 7$) mice were intratracheally infected with *M. tuberculosis* H37Rv (1×10^6 CFU). At 6 wk after infection, homogenates of the lungs and livers were plated on 7H10-OADC agar and the CFU titers were counted. Symbols represent individual mice, and bars represent the mean CFU numbers. *, $p < 0.05$; **, $p < 0.005$. Data are representative of two independent experiments. *C*, H&E staining of representative lung tissues from wild-type and *Lcn2*$^{-/-}$ mice at 20 days after intratracheal infection with *M. tuberculosis*.

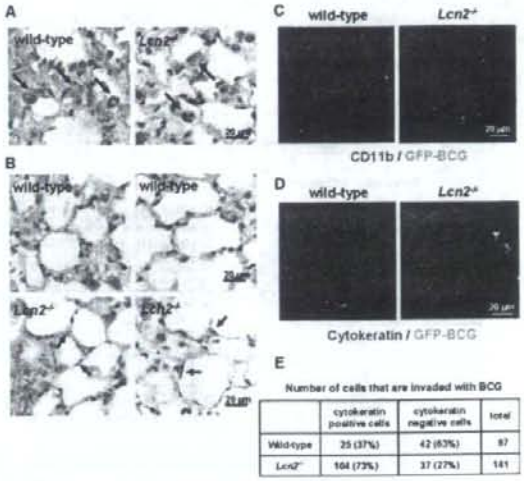

FIGURE 4. Increased numbers of *M. tuberculosis* in *Lcn2*$^{-/-}$ alveolar epithelial cells. *A* and *B*, Wild-type and *Lcn2*$^{-/-}$ mice were intratracheally infected with *M. tuberculosis* H37Ra. At 5 days after infection, the lungs were fixed in paraffin, sectioned, and stained with the Ziehl-Neelsen method. Arrows indicate red-stained *M. tuberculosis*. *C–E*, At 5 days after intratracheal infection with GFP-expressing BCG (green), lung tissue sections were stained with anti-CD11b Ab (*C*, red) or anti-pan-cytokeratin Ab (*D*, red), and visualized by fluorescence microscopy. The number of cells containing BCG was counted in a total of ten areas of pictures that visualized different fields (*E*).

Increased numbers of mycobacteria in Lcn2-deficient alveolar epithelial cells

We next analyzed the localization of *M. tuberculosis* in the lungs at 5 days after intratracheal infection by staining acid-fast bacilli using the Ziehl-Neelsen method. In wild-type and *Lcn2*$^{-/-}$ mice, similar densities of *M. tuberculosis* were observed in granulomatous lesions, although the number and size of the granulomatous lesions were increased in *Lcn2*$^{-/-}$ mice (data not shown). In addition, *M. tuberculosis* exhibited similar staining of cells with a macrophage-like morphology in wild-type and *Lcn2*$^{-/-}$ mice (Fig. 4*A*). Strikingly, some of the alveolar epithelial cell layers in *Lcn2*$^{-/-}$ mice contained *M. tuberculosis* (Fig. 4*B*). In sharp contrast, *M. tuberculosis* was scarcely detected within the epithelial cell layers of wild-type mice. To corroborate these findings, we subjected the lungs of mice intratracheally infected with GFP-expressing BCG to immunohistochemical analyses. In both wild-type and *Lcn2*$^{-/-}$ mice, CD11b-positive cells contained GFP-expressing BCG. However, in the lungs of *Lcn2*$^{-/-}$ mice, GFP-expressing BCG was frequently observed in cells that did not express CD11b, in contrast to the low frequency observed in the lungs of wild-type mice (Fig. 4*C*). Visualization of epithelial cells using an anti-cytokeratin Ab indicated that increased numbers of alveolar epithelial cells in *Lcn2*$^{-/-}$ mice contained GFP-expressing BCG compared with those in wild-type mice (Fig. 4, *D* and *E*). Thus, in the absence of Lcn2, invasion and replication of mycobacteria in alveolar epithelial cells were increased.

Therefore, we assessed the sensitivities of alveolar macrophages and alveolar epithelial cells to in vitro infection with BCG. First, alveolar macrophages were isolated from wild-type and *Lcn2*$^{-/-}$ mice, and infected with BCG (Fig. 5*A*). The CFU titers of BCG in macrophages at 4 and 7 days after infection were comparable between wild-type and *Lcn2*$^{-/-}$ cells. Thus, the absence of Lcn2 did not affect the anti-mycobacterial activity in alveolar macrophages. Next, we established AECs from wild-type and *Lcn2*$^{-/-}$ mice. Because AECs are difficult to culture in vitro, we took advantage of transgenic mice harboring a temperature-sensitive mutation of the SV40 large tumor Ag gene under the control of an IFN-γ-inducible H-2K^b promoter element (30–32). Using these mice, we successfully established wild-type and *Lcn2*$^{-/-}$ AECs, both of which were stained with anti-SP-C Ab (data not shown). AECs from wild-type mice expressed Lcn2 mRNA and secreted Lcn2 protein into the culture medium when infected with BCG (data not shown). Thus, these AECs showed the characteristics of type II alveolar epithelial cells. AECs were infected with BCG, and the CFU titers within the cells were counted at 1, 2, 3, and 4 days after infection (Fig. 5*B*). At 3 and 4 days after infection, the CFU titers in *Lcn2*$^{-/-}$ cells were increased compared with those in wild-type cells. Addition of exogenous rLcn2 reduced the CFU numbers in *Lcn2*$^{-/-}$ cells (Fig. 5*C*). Taken together, these findings indicate that the high susceptibility of *Lcn2*$^{-/-}$ mice to *M. tuberculosis* infection is attributable to impaired clearance of mycobacteria from alveolar epithelial cells, rather than alveolar macrophages, in the absence of Lcn2.

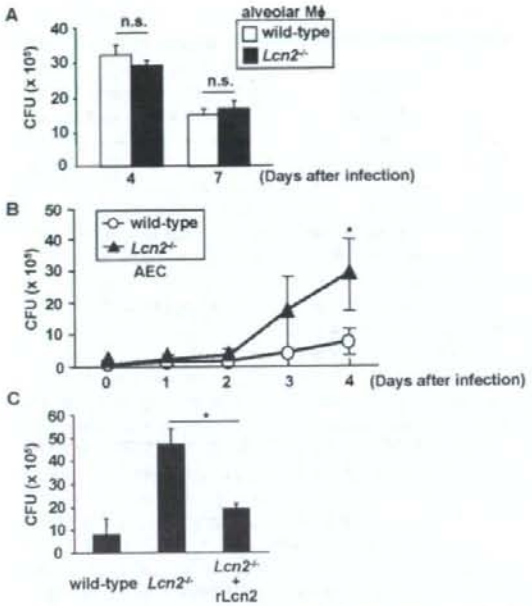

FIGURE 5. Increased BCG growth in $Lcn2^{-/-}$ alveolar epithelial cells. *A*, Alveolar macrophages were collected from uninfected wild-type and $Lcn2^{-/-}$ mice and cultured with BCG for the indicated periods. To eliminate external BCG, the cells were cultured with streptomycin for 1 h, washed three times, and harvested. Lysates of the cells were plated on 7H10-OADC agar, and the CFU numbers were counted. Representative data of two independent experiments are shown. n.s., not significant. *B*, Wild-type and $Lcn2^{-/-}$ AECs were cultured with BCG for the indicated periods. After removal of extracellular BCG, lysates the cells were plated on 7H10-OADC agar, and the CFU numbers were counted. Data are presented as means ± SD of triplicate determinations and are representative of three independent experiments. *, $p < 0.05$. Similar results were obtained when other AECs from wild-type and $Lcn2^{-/-}$ mice were used. *C*, Wild-type and $Lcn2^{-/-}$ AECs were cultured with BCG. At 2 days after infection, rLcn2 (final concentration 30 μg/ml) was added to the $Lcn2^{-/-}$ AEC. After an additional 2 days of culture, the cells were incubated with streptomycin for 1 h, washed three times, and harvested. Lysates of the cells were plated on 7H10-OADC agar, and the CFU numbers were counted. Representative data of three independent experiments are shown. Data are presented as means ± SD of triplicate determinations. *, $p < 0.05$.

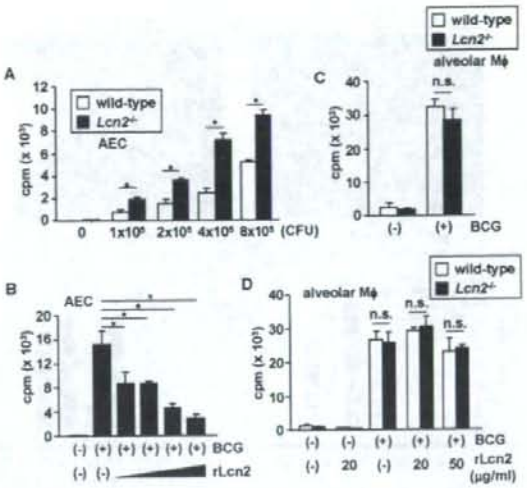

FIGURE 6. Lcn2-mediated inhibition of intracellular BCG growth. *A*, Wild-type and $Lcn2^{-/-}$ AECs were seeded onto 96-well plates and infected with the indicated CFUs of BCG for 6 h. The cells were then extensively washed to remove extracellular BCG and cultured in the presence of [^{3}H]uracil for 48 h. The incorporation of [^{3}H]uracil was measured. Data are presented as means ± SD of triplicate samples. Representative data of three independent experiments are shown. *, $p < 0.005$. *B*, $Lcn2^{-/-}$ AECs were seeded onto 96-well plates, and infected with BCG (2×10^5 CFU) for 6 h. After vigorous washing, the cells were cultured with increasing concentrations of rLcn2 (20, 30, 40, and 50 μg/ml) and [^{3}H]uracil for 48 h, before being measured for their [^{3}H]uracil incorporation. Data are presented as means ± SD of triplicate samples, and are representative of two independent experiments. * indicate a significant difference among groups, ANOVA, posthoc Scheffe, *, $p < 0.001$. *C*, Alveolar macrophages were collected from uninfected wild-type and $Lcn2^{-/-}$ mice, and cultured with BCG for 6 h. After vigorous washing, the cells were cultured in the presence of [^{3}H]uracil for 48 h, before being measured for their [^{3}H]uracil incorporation. Data are presented as the mean ± SD of triplicate samples. n.s., not significant. *D*, Alveolar macrophages from wild-type and $Lcn2^{-/-}$ mice were infected with BCG for 6 h. After vigorous washing, the cells were cultured in the presence of the indicated concentration of rLcn2 and [^{3}H]uracil for 48 h. Then, the [^{3}H]uracil incorporation was counted. Data are presented as means ± SD of triplicate samples. n.s., not significant.

Inhibition of intracellular mycobacterial growth by Lcn2

Mycobacteria are intracellular bacteria that replicate within cells. In the experiments performed so far, it is possible that extracellular growth was monitored as well as intracellular growth under the in vitro conditions. Therefore, to assess the intracellular growth of mycobacteria more precisely, we used [^{3}H]uracil, which is preferentially incorporated into mycobacterial nucleic acids (33). AECs derived from wild-type and $Lcn2^{-/-}$ mice were infected with several CFUs of BCG for 6 h, extensively washed with culture medium containing streptomycin to exclude extracellular BCG, and then cultured for 2 days in the presence of [^{3}H]uracil (Fig. 6*A*). Under these conditions, [^{3}H]uracil incorporation was below 1×10^2 cpm in wells containing uninfected AECs or wells placed in contact with BCG and then extensively washed. After infection with each CFU, [^{3}H]uracil incorporation was increased in $Lcn2^{-/-}$ cells compared with wild-type cells. In BCG-infected $Lcn2^{-/-}$ cells, addition of exogenous rLcn2 reduced the uptake of [^{3}H]uracil by intracellular BCG (Fig. 6*B*). In alveolar macrophages, the [^{3}H]uracil incorporation by intracellular BCG was comparable between wild-type and $Lcn2^{-/-}$ cells (Fig. 6*C*). Addition of rLcn2 did not effectively reduce the uptake of [^{3}H]uracil by intracellular BCG in alveolar macrophages from both wild-type and $Lcn2^{-/-}$ mice (Fig. 6*D*). These findings indicate that extracellular Lcn2 limits intracellular growth of BCG in AECs, but not in alveolar macrophages.

Because extracellular Lcn2 modulated intracellular mycobacterial growth in the AECs, we analyzed whether extracellular Lcn2 was incorporated into the AECs as described in several previous reports (18, 19). AECs were infected with GFP-expressing BCG and then treated with fluorescein-labeled rLcn2 (Fig. 7*A*). Lcn2 was detected within the AECs, and colocalized with dextran that was taken up into the cells by endocytosis. Furthermore, many BCG were colocalized with rLcn2, indicating that endocytosed Lcn2 was in close proximity to intracellular BCG. In contrast, although Lcn2 was incorporated into alveolar macrophages, the incorporated Lcn2 was not colocalized with BCG in alveolar macrophages (Fig. 7*B*), indicating that BCG and rLcn2 were localized in distinct cellular compartments within macrophages. We blocked

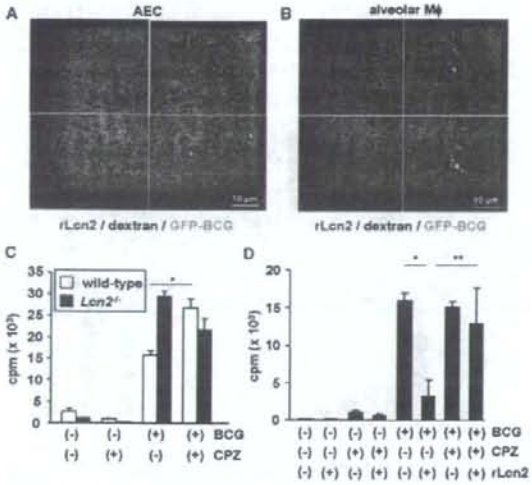

FIGURE 7. Requirement of Lcn2 incorporation for the inhibition of intracellular BCG growth. *A*, GFP-expressing BCG (green)-infected alveolar epithelial cells were cultured with dextran (25 μg/ml; blue) and fluorescein-labeled rLcn2 (15 μg/ml; red) for 6 h. The cells were then washed, fixed with 4% PFA, and analyzed by confocal microscopy. Data are representative of three independent experiments. *B*, GFP-expressing BCG (green)-infected alveolar macrophages were cultured with dextran (25 μg/ml; blue) and fluorescein-labeled rLcn2 (15 μg/ml; red) for 6 h. The cells were then washed, fixed with 4% PFA for 5 min, and analyzed by confocal microscopy. *C*, Wild-type and *Lcn2*$^{-/-}$ AECs were seeded onto 96-well plates and infected with BCG (2×10^5 CFU) for 6 h. After extensive washing, the cells were cultured with CPZ (10 μM) and [^{3}H]uracil for 48 h. The [^{3}H]uracil incorporation was then measured. Data are presented as means ± SD of triplicate samples, and are representative of two independent experiments. *, $p < 0.01$. *D*, *Lcn2*$^{-/-}$ AECs were seeded onto 96-well plates, and infected with BCG for 6 h. After washing, the cells were cultured with CPZ for 30 min and then cultured with rLcn2 (20 μg/ml) and [^{3}H]uracil for 48 h. The [^{3}H]uracil incorporation was measured. Data are presented as means ± SD of triplicate samples, and are representative of two independent experiments. * or ** indicate a significant difference among groups, ANOVA, posthoc Scheffe, *, $p < 0.005$; **, $p < 0.05$.

endocytosis of Lcn2 using CPZ after BCG infection. Addition of CPZ resulted in increased BCG growth in wild-type AECs, but not in *Lcn2*$^{-/-}$ cells (Fig. 7*C*). We also analyzed the effects of the endocytosis inhibitor on rLcn2-mediated inhibition of BCG growth (Fig. 7*D*). Addition of CPZ abolished Lcn2-mediated inhibition of [^{3}H]uracil incorporation in both wild-type and *Lcn2*$^{-/-}$ cells. Cytochalasin B, which also blocks endocytosis, had similar effects to those of CPZ on Lcn2-mediated inhibition of intracellular BCG growth (data not shown). These findings indicate that endocytosed Lcn2 inhibits the intracellular growth of BCG in AECs.

Discussion

Lcn2 has a variety of putative functions, as evident from its many different names such as neutrophil gelatinase-associated lipocalin, uterocalin, 24p3, and siderocalin (12, 13, 16, 19). In the context of its function in host defense, a structural study of the Lcn2 protein revealed that it associates with enterobactin-type bacterial siderophores (16). Subsequently, Lcn2 was shown to bind to several types of siderophores such as caroboxy-mycobactin and bacillibactin (20, 21). In addition, Lcn2 has been proposed to bind to an as-yet unknown mammalian siderophore (18, 34). Thus, Lcn2 has the ability to bind to a variety of types of siderophores. Furthermore, Lcn2 has been shown to inhibit the growth of *E. coli* through sequestration of iron uptake (22, 23). The present study has demonstrated that Lcn2 also participates in the inhibition of mycobacterial growth through similar mechanisms to those against *E. coli*. Indeed, Lcn2 has been shown to associate with the mycobacteria-derived hydrophilic siderophore carboxy-mycobactin (21). In accordance with our results, Lcn2 has been shown to be secreted from neutrophils during *M. tuberculosis* infection and inhibit their growth (35). Lcn2 was originally identified as a molecule that is secreted from neutrophils, which are rapidly recruited to *M. tuberculosis*-infected lungs. Therefore, neutrophils are presumably the source of Lcn2 as well as alveolar macrophages and epithelial cell during *M. tuberculosis* infection.

Regarding the high sensitivity of *Lcn2*$^{-/-}$ mice to *M. tuberculosis* infection, it is noteworthy that *Lcn2*$^{-/-}$ alveolar epithelial cells, but not macrophages, contained increased numbers of *M. tuberculosis* at the early phase of the infection, as evaluated by histopathological and immunohistochemical analyses. This finding was unexpected, because successful in vivo detection of mycobacteria in respiratory epithelial cells in wild-type mice has only been achieved through analyses of mycobacterial DNA or use of electron microscopy, even though mycobacteria have been shown to invade epithelial cells as well as macrophages in vitro (6–9, 36). In addition, *Lcn2*$^{-/-}$ alveolar epithelial cells, but not macrophages, exhibited defective inhibition of intracellular mycobacterial growth, suggesting that impaired inhibition of mycobacterial growth in alveolar epithelial cells due to the absence of Lcn2 may be a major cause of the high susceptibility *Lcn2*$^{-/-}$ mice to *M. tuberculosis* infection. Given that mycobacteria were easily detected in the alveolar epithelial cell layers by a typical histological approach in the absence of Lcn2 and the increased mycobacterial growth was observed in *Lcn2*$^{-/-}$ epithelial cells, but not in macrophages, epithelial cells may play an important role in the host immune responses against respiratory infection with *M. tuberculosis*.

Mycobacteria replicate within cells in vivo, and several lines of evidence indicate that mycobactin-mediated iron uptake is a prerequisite for intracellular mycobacterial growth (27, 29). Consistent with previous studies (18, 19), our findings indicated that Lcn2 is internalized into alveolar epithelial cells via endocytosis. Furthermore, addition of rLcn2 effectively inhibited intracellular mycobacterial growth in AECs, and this effect was abolished by endocytosis inhibitors. At present, it remains unclear how mycobacteria take up iron within epithelial cells using mycobactin. First, it is apparent that mycobacteria exist in the phagosome of macrophages. However, the subcellular localization of mycobacteria within epithelial cells has not been established, although mycobacteria have been shown to be localized in endosomes or macropinosomes (37, 38). Our results revealed colocalization of mycobacteria and dextran, indicating that mycobacteria exist in the endosome-like vacuole within epithelial cells. Second, it remains obscure whether mycobacteria secrete water-soluble carboxy-mycobactin into the cytoplasm to bind the cytosolic iron. It is also obscure how endocytosed Lcn2 approaches the carboxy-mycobactin/iron complexes within the cells. Given that Lcn2 and mycobacteria are colocalized within the endosome-like structure, it is possible that mycobacteria take up the iron entering the endosome using mycobactin, and endocytosed Lcn2, in turn, binds to the carboxy-mycobactin/iron complexes, thereby blocking iron acquisition by mycobacteria. Further studies are required to clarify the precise mechanisms for the interaction between Lcn2 and mycobacteria-derived carboxy-mycobactin.

In alveolar macrophages, the absence of Lcn2 did not affect the sensitivity to mycobacterial infection. This may be due to the differential localizations of mycobacteria in epithelial cells and macrophages. Lcn2 was colocalized with mycobacteria in epithelial

cells, indicating that mycobacteria exist within the endosome-like structure. In contrast, mycobacteria were localized within the phagosome in macrophages, leading to distinct localizations of Lcn2 and mycobacteria in macrophages. Alternatively, macrophages are professional cells that kill intracellular bacteria by producing several macrophage-specific anti-microbial mediators, including NO synthase and Nramp1 (39–41). These mediators may compensate the Lcn2 deficiency in macrophages. In contrast, they are not expressed in epithelial cells, resulting in the high sensitivity to mycobacterial infection in the absence of Lcn2. Thus, in alveolar epithelial cells, Lcn2 may be a major factor that mediates host resistance to mycobacterial infection.

Our results highlight a novel innate host defense system that inhibits mycobacterial infection at the respiratory mucosal surface. We would like to propose the following scenario with regard to the function of Lcn2. Lcn2 is secreted into the alveolar space by alveolar macrophages and epithelial cells during the early phase of respiratory mycobacterial infection. Lcn2 presumably inhibits mycobacterial growth within the alveolar space. In addition, Lcn2 is internalized into the alveolar epithelial cells, which are invaded by mycobacteria, and inhibits mycobacterial growth by sequestering iron uptake. This leads to a reduction in the number of infected mycobacteria at the early phase of infection, which may help to create sufficient time for effective activation of anti-mycobacterial innate and adaptive immune responses. Thus, respiratory epithelial cells play an active role in the resistance to mycobacterial infection, in addition to their functions as physical barriers and secretors of anti-bacterial mediators.

Acknowledgments

We thank I. Sugawara for providing the *M. tuberculosis* H37Rv, Y. Yamada and K. Takeda for technical assistance, and M. Kurata and M. Yasuda for secretarial assistance.

Disclosures

The authors have no financial conflict of interest.

References

1. North, R. J., and Y. J. Jung. 2004. Immunity to tuberculosis. *Annu. Rev. Immunol.* 22: 599–623.
2. Kaufmann, S. H. 2006. Tuberculosis: back on the immunologists' agenda. *Immunity* 24: 351–357.
3. Quesniaux, V., C. Fremond, M. Jacobs, S. Parida, D. Nicolle, V. Yeremeev, F. Bihl, F. Erard, T. Botha, M. Drennan, et al. 2004. Toll-like receptor pathways in the immune responses to mycobacteria. *Microbes Infect.* 6: 946–959.
4. Fremond, C. M., V. Yeremeev, D. M. Nicolle, M. Jacobs, V. F. Quesniaux, and B. Ryffel. 2004. Fatal *Mycobacterium tuberculosis* infection despite adaptive immune response in the absence of MyD88. *J. Clin. Invest.* 114: 1790–1799.
5. Aoki, K., S. Matsumoto, Y. Hirayama, T. Wada, Y. Ozeki, M. Niki, P. Domenech, K. Umemori, S. Yamamoto, A. Mineda, et al. 2004. Extracellular mycobacterial DNA-binding protein 1 participates in mycobacterium-lung epithelial cell interaction through hyaluronic acid. *J. Biol. Chem.* 279: 39798–39806.
6. Teitelbaum, R., W. Schubert, L. Gunther, Y. Kress, F. Macaluso, J. W. Pollard, D. N. McMurray, and B. R. Bloom. 1999. The M cell as a portal of entry to the lung for the bacterial pathogen *Mycobacterium tuberculosis*. *Immunity* 10: 641–651.
7. Bermudez, L. E., and F. J. Sangari. 2001. Cellular and molecular mechanisms of internalization of mycobacteria by host cells. *Microbes Infect.* 3: 37–42.
8. Bermudez, L. E., F. J. Sangari, P. Kolonoski, M. Petrofsky, and J. Goodman. 2002. The efficiency of the translocation of *Mycobacterium tuberculosis* across a bilayer of epithelial and endothelial cells as a model of the alveolar wall is a consequence of transport within mononuclear phagocytes and invasion of alveolar epithelial cells. *Infect. Immun.* 70: 140–146.
9. Hernandez-Pando, R., M. Jeyanathan, G. Mengistu, D. Aguilar, H. Orozco, M. Harboe, G. A. Rook, and G. Bjune. 2000. Persistence of DNA from *Mycobacterium tuberculosis* in superficially normal lung tissue during latent infection. *Lancet* 356: 2133–2138.
10. Ferguson, J. S., and L. S. Schlesinger. 2000. Pulmonary surfactant in innate immunity and the pathogenesis of tuberculosis. *Tuber. Lung Dis.* 80: 173–184.
11. Kjeldsen, L., J. B. Cowland, and N. Borregaard. 2000. Human neutrophil gelatinase-associated lipocalin and homologous proteins in rat and mouse. *Biochim. Biophys. Acta* 1482: 272–283.
12. Devireddy, L. R., J. G. Teodoro, F. A. Richard, and M. R. Green. 2001. Induction of apoptosis by a secreted lipocalin that is transcriptionally regulated by IL-3 deprivation. *Science* 293: 829–834.
13. Kjeldsen, L., A. H. Johnsen, H. Sengelov, and N. Borregaard. 1993. Isolation and primary structure of NGAL, a novel protein associated with human neutrophil gelatinase. *J. Biol. Chem.* 268: 10425–10432.
14. Flower, D. R., A. C. North, and T. K. Attwood. 1991. Mouse oncogene protein 24p3 is a member of the lipocalin protein family. *Biochem. Biophys. Res. Commun.* 180: 69–74.
15. Liu, Q., J. Ryon, and M. Nilsen-Hamilton. 1997. Uterocalin: a mouse acute phase protein expressed in the uterus around birth. *Mol. Reprod. Dev.* 46: 507–514.
16. Goetz, D. H., M. A. Holmes, N. Borregaard, M. E. Bluhm, K. N. Raymond, and R. K. Strong. 2002. The neutrophil lipocalin NGAL is a bacteriostatic agent that interferes with siderophore-mediated iron acquisition. *Mol. Cell* 10: 1033–1043.
17. Nilsen-Hamilton, M., Q. Liu, J. Ryon, L. Bendickson, P. Lepont, and Q. Chang. 2003. Tissue involution and the acute phase response. *Ann. NY Acad. Sci.* 995: 94–108.
18. Devireddy, L. R., C. Gazin, X. Zhu, and M. R. Green. 2005. A cell-surface receptor for lipocalin 24p3 selectively mediates apoptosis and iron uptake. *Cell* 123: 1293–1305.
19. Yang, J., D. Goetz, J. Y. Li, W. Wang, K. Mori, D. Setlik, T. Du, H. Erdjument-Bromage, P. Tempst, R. Strong, and J. Barasch. 2002. An iron delivery pathway mediated by a lipocalin. *Mol. Cell* 10: 1045–1056.
20. Abergel, R. J., M. K. Wilson, J. E. Arceneaux, T. M. Hoette, R. K. Strong, B. R. Byers, and K. N. Raymond. 2006. Anthrax pathogen evades the mammalian immune system through stealth siderophore production. *Proc. Natl. Acad. Sci. USA* 103: 18499–18503.
21. Holmes, M. A., W. Paulsene, X. Jide, C. Ratledge, and R. K. Strong. 2005. Siderocalin (Lcn 2) also binds carboxymycobactins, potentially defending against mycobacterial infections through iron sequestration. *Structure* 13: 29–41.
22. Flo, T. H., K. D. Smith, S. Sato, D. J. Rodriguez, M. A. Holmes, R. K. Strong, S. Akira, and A. Aderem. 2004. Lipocalin 2 mediates an innate immune response to bacterial infection by sequestrating iron. *Nature* 432: 917–921.
23. Berger, T., A. Togawa, G. S. Duncan, A. J. Elia, A. You-Ten, A. Wakeham, H. E. Fong, C. C. Cheung, and T. W. Mak. 2006. Lipocalin 2-deficient mice exhibit increased sensitivity to *Escherichia coli* infection but not to ischemia-reperfusion injury. *Proc. Natl. Acad. Sci. USA* 103: 1834–1839.
24. Smith, K. D. 2007. Iron metabolism at the host pathogen interface: lipocalin 2 and the pathogen-associated iroA gene cluster. *Int. J. Biochem. Cell Biol.* 39: 1776–1780.
25. Houben, E. N., L. Nguyen, and J. Pieters. 2006. Interaction of pathogenic mycobacteria with the host immune system. *Curr. Opin. Microbiol.* 9: 76–85.
26. De Voss, J. J., K. Rutter, B. G. Schroeder, and C. E. Barry, 3rd. 1999. Iron acquisition and metabolism by mycobacteria. *J. Bacteriol.* 181: 4443–4451.
27. De Voss, J. J., K. Rutter, B. G. Schroeder, H. Su, Y. Zhu, and C. E. Barry, 3rd. 2000. The salicylate-derived mycobactin siderophores of *Mycobacterium tuberculosis* are essential for growth in macrophages. *Proc. Natl. Acad. Sci. USA* 97: 1252–1257.
28. Gobin, J., and M. A. Horwitz. 1996. Exochelins of *Mycobacterium tuberculosis* remove iron from human iron-binding proteins and donate iron to mycobactins in the *M. tuberculosis* cell wall. *J. Exp. Med.* 183: 1527–1532.
29. Luo, M., E. A. Fadeev, and J. T. Groves. 2005. Mycobactin-mediated iron acquisition within macrophages. *Nat. Chem. Biol.* 1: 149–153.
30. Jat, P. S., M. D. Noble, P. Ataliotis, Y. Tanaka, N. Yannoutsos, L. Larsen, and D. Kioussis. 1991. Direct derivation of conditionally immortal cell lines from an H-2Kb-tsA58 transgenic mouse. *Proc. Natl. Acad. Sci. USA* 88: 5096–5100.
31. Whitehead, R. H., P. E. VanEeden, M. D. Noble, P. Ataliotis, and P. S. Jat. 1993. Establishment of conditionally immortalized epithelial cell lines from both colon and small intestine of adult H-2Kb-tsA58 transgenic mice. *Proc. Natl. Acad. Sci. USA* 90: 587–591.
32. deMello, D. E., S. Mahmoud, P. J. Padfield, and J. W. Hoffmann. 2000. Generation of an immortal differentiated lung type-II epithelial cell line from the adult H-2K(b)tsA58 transgenic mouse. *In Vitro Cell. Dev. Biol. Anim.* 36: 374–382.
33. Rook, G. A., B. R. Champion, J. Steele, A. M. Varey, and J. L. Stanford. 1985. I-A restricted activation by T cell lines of anti-tuberculosis activity in murine macrophages. *Clin. Exp. Immunol.* 59: 414–420.
34. Mori, K., H. T. Lee, D. Rapoport, I. R. Drexler, K. Foster, J. Yang, K. M. Schmidt-Ott, X. Chen, J. Y. Li, S. Weiss, et al. 2005. Endocytic delivery of lipocalin-siderophore-iron complex rescues the kidney from ischemia-reperfusion injury. *J. Clin. Invest.* 115: 610–621.
35. Martineau, A. R., S. M. Newton, K. A. Wilkinson, B. Kampmann, B. M. Hall, N. Nawroly, G. E. Packe, R. N. Davidson, C. J. Griffiths, and R. J. Wilkinson. 2007. Neutrophil-mediated innate immune resistance to mycobacteria. *J. Clin. Invest.* 117: 1988–1994.
36. Sato, K., H. Tomioka, T. Shimizu, T. Gonda, F. Ota, and C. Sano. 2002. Type II alveolar cells play roles in macrophage-mediated host innate resistance to pulmonary mycobacterial infections by producing proinflammatory cytokines. *J. Infect. Dis.* 185: 1139–1147.
37. Bermudez, L. E., and J. Goodman. 1996. *Mycobacterium tuberculosis* invades and replicates within type II alveolar cells. *Infect. Immun.* 64: 1400–1406.
38. Garcia-Perez, B. E., R. Mondragon-Flores, and J. Luna-Herrera. 2003. Internalization of *Mycobacterium tuberculosis* by macropinocytosis in non-phagocytic cells. *Microb. Pathog.* 35: 49–55.
39. Adams, D. O., and T. A. Hamilton. 1984. The cell biology of macrophage activation. *Annu. Rev. Immunol.* 2: 283–318.
40. MacMicking, J., Q. W. Xie, and C. Nathan. 1997. Nitric oxide and macrophage function. *Annu. Rev. Immunol.* 15: 323–350.
41. Govoni, G., and P. Gros. 1998. Macrophage NRAMP1 and its role in resistance to microbial infections. *Inflamm. Res.* 47: 277–284.

遺伝子を用いた抗酸菌鑑別同定試薬 INNO-LiPA MYCOBACTERIA v2の有用性の検討

[1]吉田志緒美 [1]鈴木 克洋 [1]露口 一成 [4]岩本 朋忠
[2]富田 元久 [1]岡田 全司 [3]坂谷 光則

要旨:〔目的〕遺伝子を用いた抗酸菌鑑別用同定試薬INNO-LiPA MYCOBACTERIA v2（INNO-LiPA法）のわが国における有用性の検討。〔対象〕NHO近畿中央胸部疾患センターにおいて新規に分離された抗酸菌122株。〔方法〕INNO-LiPA法と3種類の同定キット（コバス アンプリコア マイコバクテリウム法，アキュプローブ法とDDH法）との結果を比較検討した。同定不能もしくはデータ間で違う結果を示した株についてはシークエンス解析を行った。〔結果〕122株のうち112株が3種類の同定キットのいずれかとINNO-LiPA法の結果が一致した（91.8%）。相違を認めた10株のうち6株はINNO-LiPA法とシークエンス解析の結果が一致した。しかし2株のうち1株はDDH法の結果と一致し*M. fortuitum*，もう1株はコバス アンプリコア マイコバクテリウム法とアキュプローブMAC法の結果と一致し*M. intracellulare*と判定された。INNO-LiPA法と3種類の同定キットの結果がともにシークエンス解析結果と異なる株は2株認められた（*M. paraffinicum*，*M. mucogenicum*近縁種）。〔考察〕INNO-LiPA法は正確性，迅速性に優れており有益性が証明された。培養および生化学的性状試験と併行して実施することにより総合的な抗酸菌同定が可能であると考えられた。

キーワーズ：抗酸菌，INNO-LiPA MYCOBACTERIA v2，同定検査，16S rRNA遺伝子，ITSシークエンス解析

はじめに

抗酸菌同定検査において生化学的同定検査を実施するには多大な労力と菌量が必要である。また培養にかかる期間も結核菌だと小川培地で3～8週間は必要であり，治療方針を決定するうえでも迅速な同定検査は必須である。近年，遺伝子検査の手法を応用した抗酸菌の迅速同定検査が日常的に用いられるようになり，さまざまな測定原理から開発された菌同定用キットが市販されている。抗酸菌を正確かつ迅速に同定する性能を兼ね備えたこれらのキットは，先人により高い評価と共に各種問題点も報告されている[1)~7)]。

コバス アンプリコア マイコバクテリウム法はpolymerase chain reaction（PCR）を用いてDNAを増幅後，ハイブリダイゼーションすることで臨床検体や菌株を対象として*M. tuberculosis* complex，*M. avium*，*M. intracellulare*の3菌種が同定できる[1)~3)]。前倉らによると肺結核患者における塗抹陽性検体の94.4%はコバス アンプリコア マイコバクテリウム法で陽性であったが，塗抹陰性検体の場合は70.8%が陽性となった[4)]。

アキュプローブ法は検体の16S rRNAをターゲットとして，菌種特異的DNAプローブとハイブリダイゼーションさせてから，専用の検出器を用いて化学発光を検出するキットである[5)]。結核菌群と*M. avium* complex（MAC），*M. kansasii*，*M. gordonae*の4種類のキットがあり，アキュプローブ陽性となる感度は結核菌群と*M. gordonae*で100%，MAC 95.2%，*M. kansasii* 44.0%という報告[5)]や，結核菌群87.2%，MAC 78.6%，*M. kansasii* 91.7%，*M. gordonae* 85.9%とする報告[6)]などがある。

DDH法は核酸の相同性を利用し，ハイブリダイズし

独立行政法人国立病院機構近畿中央胸部疾患センター[1]臨床研究センター，[2]研究検査科，[3]内科，[4]神戸市環境保健研究所

連絡先：吉田志緒美，独立行政法人国立病院機構近畿中央胸部疾患センター臨床研究センター，〒591-8555 大阪府堺市北区長曽根町1180（E-mail: dustin@kch.hosp.go.jp）
（Received 28 Aug. 2008/Accepted 30 Oct. 2008）

たDNAの比率をビオチン-アビジン反応を用いてそれぞれの基準DNA株と被検菌DNAのDNA塩基配列の相同性を測定するキットで18菌種の同定を一度に行うことが可能である[7]。同法は「全染色体DNAの類似度(similarity)が70%以上であれば，同じ菌種としてよい」という細菌分類学の菌種同定基準を利用している。そのため相対類似度で算出された数値から供試菌がどの菌種の基準株に最も近いかという結果は得られるが，同定不能となる菌種が多い傾向がある[8][9]。また「肉眼的に明らかな発色が確認された場合には吸光度を測定せずにウェルの菌種と同定してもよい」としていることも誤判定を生じやすい原因である。

INNO-LiPA MYCOBACTERIA v2（INNO-LiPA法）は16S-23S internal transcribed spacer（ITS）領域をターゲットとしPCR法で増幅されたDNAを対象に，ラインプローブアッセイを用いて検出する。一度に15菌種の同定と*Mycobacterium*属に共通の*Mycobacterium* genusのプローブがあることから抗酸菌の確定が可能である[10]。

INNO-LiPA法の検討はこれまでにいくつか報告はあるが[10]~[13]，現時点でわが国における検討報告はなされていない。今回われわれはINNO-LiPA法の迅速性ならびに正確性について上記の先に市販されている同定キットの結果と比較しその有用性を検討した。

方　法

対象

独立行政法人近畿中央胸部疾患センターにおいて新規に分離培養される菌株のうち大半を占める抗酸菌は結核菌群であるが，多くの菌種が存在し，日常検査で判定に苦慮する割合が高いのは非結核性抗酸菌（NTM）である。今回NTMに対する同定結果の比較に重点をおき，結核菌群の菌株数を絞って検討を試みた。したがって2006年2月1日から6月30日までの期間に分離された結核菌群7株，NTM 115株の合計122株を対象とした。すべての菌株同定は同定検査結果とあわせて小川培地上でのコロニー性状の観察をもって最終判定とした。

検体内に複数の菌が混在する場合に同時に鑑別が可能かどうかを検討するため，臨床検体から複数の菌種が認められた3つの混合培養も検討に加えた。これらはあらかじめ固形培地上で異なるコロニー性状をもつと判定され，おのおのに純培養を行って3種類の同定キットにて同定検査を実施，複数菌混在であることを確認した。

同定キット

NHO近畿中央胸部疾患センターにおいて日常検査に使用している遺伝子を用いた同定キットを使用した。

結核菌群の同定には結核菌群同定用アキュプローブ結核菌群同定キット（極東製薬工業）と結核菌群同定試薬キャピリアTB（日本ベクトン・ディッキンソン）を用いた。*M. avium*と*M. intracellulare*の同定にはコバス アンプリコア マイコバクテリウム アビウムとコバス アンプリコア マイコバクテリウム イントラセルラー（コバス アンプリコア マイコバクテリウム法：ロシュ・ダイアグノスティクス），MACの同定にはアキュプローブ マイコバクテリウム アビウム コンプレックス（アキュプローブMAC法：極東製薬工業）を用いた。*M. kansasii*および*M. gordonae*の同定には，研究用試薬であるアキュプローブ マイコバクテリウム カンサシとアキュプローブ マイコバクテリウム ゴルドネ（共に極東製薬工業）を用いた。上記以外の菌種の同定にはDDHマイコバクテリア‘極東’（DDH法：極東製薬工業）を用いた。すべての方法は添付の仕様説明書に準拠して行った。DDH法はDNAの精製が不十分な場合に同定不能の結果が得られることもあるため同定不能の結果が得られた場合には再検査を行った。

DNAの抽出

小川培地発育菌から白金耳で径2～3 mmのコロニー2個分の菌量を採取し，1.5 mlマイクロチューブに分注したインスタジーンDNA精製マトリックス（BIO-RAD）200 μlに懸濁した。56℃，15~30分処理後10秒間vortexし，正確に100℃，8分間処理した後直ちに氷水中で急冷した。10秒間vortexし，12000 rpm，3分遠心した上清をINNO-LiPA法ならびにシークエンス解析法に用いた。

INNO-LiPA法

INNO-LiPA MYCOBACTERIA v2（INNO-LiPA法：INNOGENETICS）は，発色確認用コントロールと抗酸菌特異的プローブ（MYC genus）および菌種鑑別のための22本のITS遺伝子プローブが固相化されたストリップ状のキットである。プローブは12菌種のプローブに加えて，3種類のsubtypeが鑑別可能な*M. kansasii*プローブ，4種類のMAIS complexプローブ，*M. abscessus*を含んだ3種類の*M. chelonae* complexプローブが配置されている。同キットの使用説明書に準拠して16S-23S ITS領域の遺伝子のPCR増幅を行い，得られたPCR増幅産物をLiPA検体として使用した。LiPA検体をハイブリダイズさせ，得られた発色パターンによって抗酸菌の同定を行った（Table 1）。

INNO-LiPA法においてはPCRの後，すべてのPCR産物を電気泳動し得られたバンドから増幅の確認を行った。またDDH法と同様にMYC genusにしか発色が見られない場合，再検査を行った。

16S rRNA遺伝子，ITS領域のシークエンス解析

3種類の同定キットとINNO-LiPA法により同定不能であった株，ならびに結果の乖離が認められた株に対し

Table 1 Interpretation of *Mycobacterium* species by using the INNO-LiPA MYCOBACTERIA v2

Line	Probe	Taxa reacting with the probe
1	Conjugate Control	
2	MYC genus	Presence of *Mycobacterium* in the test sample
3	MTB	*M. tuberculosis* complex: *M. tuberculosis*, *M. bovis*, *M. microti*, *M. africanum*
4	MKA-1	*M. kansasii* (group I)*
5	MKA-2	*M. kansasii* (group II)*
6	MKA-3	*M. kansasii* (group III, V, VI)*, *M. gastri*
7	MXE	*M. xenopi*
8	MGO	*M. gordonae*
9	MGV	*M. genavense*
10	MSI	*M. simiae*
11	MMU	*M. marinum*+*M. ulcerans*
12	MCE	*M. celatum*
13	MAIS	*M. avium*, *M. intracellulare*, *M. scrofulaceum*, MAC, *M. malmoense*
14	MAV	*M. avium*, *M. paratuberculosis*, *M. silvaticum*
15	MIN-1	*M. intracellulare* (sqv. Min-A, -B, -C, and-D)
16	MIN-2	*M. intracellulare* (sqv. Mac-A)
17	MSC	*M. scrofulaceum*
18	MML	*M. malmoense*
19	MHP	*M. haemophilum*
20	MCH-1	*M. chelonae* complex (group I, II, III, IV, *M. abscessus*)*
21	MCH-2	*M. chelonae* complex (group III, *M. abscessus*)*
22	MCH-3	*M. chelonae* complex (group I)*
23	MFO	*M. fortuitum*–*M. peregrinum* complex
24	MSM	*M. smegmatis*

*group is based on sequevar derived from 16S–23S nucleotide sequences. sqv., sequevar

て，データベースが豊富な16S rRNA遺伝子のシークエンスを，さらに16S rRNA遺伝子の相同性解析で同定が困難な菌株に対してはITSシークエンス解析を追加し菌種を決定した。PCR反応は岩本らの方法[14]に準じ，Takara Ex Taq（タカラバイオ）を用いて，94℃ 30秒，55℃ 30秒，72℃ 1分を35サイクル行った。16S rRNA遺伝子の超可変部AとBを含む領域をプライマー 285F［5'-GAG AGT TTG ATC CTG GCT CAG-3'］と264R［5'-TGC ACA CAG GCC ACA AGG GA-3'］を用いてPCR増幅産物を得た。ITS領域全長の増幅にはITS1［5'-GAT TGG GAC GAA GTC GTA AC-3'］とITS2［5'-AGC CTC CCA CGT CCT TCA TC-3'］を用いた。PCR産物を精製した後BigDye Terminator Ready Reaction Cycle Sequencing Kit（Applied Biosystems Japan）を用いて16S rRNA遺伝子の部分配列とITS全長の塩基配列を得た。得られた塩基配列は，Ribosomal Differentiation of Microorganisms: RIDOMを用いて相同性検索を行い，99%以上の塩基配列一致をもって同一菌種と決定した。

結　果

供試菌122株のうち112株においてINNO-LiPA法と3種類の同定キットの結果が一致した。対象菌株のうち結核菌群の7株はすべて，結核菌群同定用アキュプローブ結核菌群同定キット，キャビリアTBとINNO-LiPA法の結果が一致した。NTM 115株のうちアキュプローブMAC法でMACと同定され，コバス アンプリコア マイコバクテリウム法により*M. avium*と同定された24株はINNO-LiPA法ではMAISとMAVプローブのバンドを認めた。一方アキュプローブMAC法でMAC，コバス アンプリコア マイコバクテリウム法により*M. intracellulare*と同定された7株がMAISとMIN-1プローブに反応していたが，菌株23のみMIN-1に反応を示さず結果に乖離が見られた。DDH法を実施した83株のうち再検査を実施しても同定不能となった株は6株認められた。これら6株のうち3株はINNO-LiPA法でもMYC genusにしか反応が見られなかった。一方DDH法で菌種同定ができたがINNO-LiPA法との間に結果の食い違いが見られた株は3株認められた。したがって3種類の同定キットのいずれかとINNO-LiPA法との間で同定不能や結果が異なった10株に対してシークエンス解析を行った。

6株（菌株2，19，14，22，7，6）はシークエンス解析結果とINNO-LiPA法の結果が一致した。菌株2と19はINNO-LiPA法でMKA-3の反応を認め*M. kansasii* 3と判定され，シークエンス解析からそれぞれアキュプローブ カンサシで陰性となる*M. kansasii* sqv. ⅢとⅥと判定された。菌株14はINNO-LiPA法，シークエンス解析ともに*M. gordonae*と判定された。一方，菌株5と23の2株は同定キットの結果とシークエンス解析結果が一致した。菌株5は，INNO-LiPA法でMYC genusに反応が認

Table 2 Discrepant and unidentified results in identification of *Mycobacterium* species, including 9 isolates of *M. lentiflavum*.

Isolate No.	Cobas Amplicor system	AccuProbe	DDH	INNO-LiPA	16S rRNA gene		ITS	
						Identity (%)		Identity (%)
9 isolates	Negative	Negative	Unidentified**	MYC genus	*M. lentiflavum* DSM44418T	429/429 (100)		
2	Negative	Negative	Unidentified**	*M. kansasii* 3	*M. kansasii* Borste 8875/99, sqv. VI-3	441/441 (100)	*M. kansasii*, MkaF	277/277 (100)
19	Negative	Negative	Unidentified**	*M. kansasii* 3	*M. kansasii* Borste 539/99, sqv. III	440/440 (100)	*M. kansasii*, MkaC	279/279 (100)
14	Negative	NT	Unidentified**	*M. gordonae*	*M. gordonae* Borste 11340/99, sqv. III	440/440 (100)	*M. gordonae*, MgoC	270/270 (100)
22	Negative	NT	Unidentified**	MYC genus	*M. interjectum* ATCC51457T	430/430 (100)		
7	Negative	NT	Unidentified***	*M. abscessus*	*M. abscessus* or *M. chelonae* (*M. abscessus* by ITS)	428/428 (100)	*M. abscessus* DSM44196	294/294 (100)
6	Negative	NT	*M. fortuitum*	*M. chelonae*	*M. abscessus* or *M. chelonae* (*M. chelonae* by ITS)	428/428 (100)	*M. chelonae* Mche B	293/294 (99.7)
5	Negative	NT	*M. fortuitum*	MYC genus	*M. fortuitum* DSM46621T	428/428 (100)		
23	*M. intracellulare*	MAC*	NT	MAIS	*M. intracellulare* ATCC35770 sqv. III	442/442 (100)		
13	Negative	NT	Unidentified***	*M. fortuitum*	*M. mucogenicum* ATCC49650T	423/428 (98.8)		
18	Negative	NT	*M. scrofulaceum*	*M. intracellulare* 2	*M. paraffinicum* DSM44181T	439/439 (100)		

M. avium complex **slow growers ***rapid growers NT: not tested T: Type strain sqv.: sequevar

められたが菌種の特定には至らず，DDH法とシークエンス解析では *M. fortuitum* と同定された。菌株23はコバス アンプリコア マイコバクテリア法で *M. intracellulare*，アキュプローブMAC法でMAC，INNO-LiPA法でMAISと判定され，シークエンス解析で *M. intracellulare* ATCC 35770 sqv. Ⅲ（Mac-D）と100%相同と判定された。

シークエンス解析結果といずれかの方法の結果が異なった株（菌株13，18）は各々 *M. mucogenicum* 近縁種と *M. paraffinicum* と同定された。

小川培地上で遅発育菌と観察され，コバス アンプリコア マイコバクテリウム法，アキュプローブ法，DDH法でも同定不能となり，INNO-LiPA法でMYC genusにしかバンドの発色が見られなかったがシークエンス解析で *M. lentiflavum* と同定された株が9株認められた（Table 2）。

複数菌種が混在していた3混合培養はINNO-LiPA法でも複数のバンドパターンが認められた（*M. tuberculosis*＋*M. gordonae*，*M. avium*＋*M. fortuitum*，*M. kansasii*＋*M. gordonae*）。

考　察

分子遺伝学的に近縁な菌種であり16S rRNA遺伝子に違いが見られない場合，ITS領域のほうが進化速度は速いため，より多様性のある配列結果が得られる。ITS領域をターゲットとしたINNO-LiPA法はITS領域で高い多型性が知られているMACに対して4種類の亜型プローブを使って亜型判定を可能としている。菌株23はアキュプローブMAC法でMAC，コバス アンプリコア マイコバクテリウム法で *M. intracellulare*，シークエンス解析で *M. intracellulare* ATCC 35770 sqv. Ⅲ（Mac-D）と判定された。INNO-LiPA法では同タイプに対応する亜型プローブは設計されていないためにMAISプローブのみの反応となった。Lebrunらも ATCC 35770の検討で同じくMAISプローブにのみ発色が認められたと報告している[13]。したがって，ITS領域において菌種内多型性を示す菌種に対しては，シークエンス解析で相同性を確認することが重要となってくる。

シークエンス解析といずれの方法とも結果が食い違った2株のうち菌株18はアキュプローブMAC法陰性，DDH法で *M. scrofulaceum* となり，INNO-LiPA法でMAISとMIN-2に発色が見られ *M. intracellulare* sqv. Mac-Aと判定された。遅発育菌である同菌株は16S rRNA解析では100%の相同性で *M. paraffinicum* DSM 44181と判定され，同じく *M. scrofulaceum* DSM 43992とは99%の相同性が見られた。Tortoliらも *M. paraffinicum* はMAISとMIN-2に発色が見られたがアキュプローブMAC法は陰性であったと報告している[10]。一方Lebrunらはアキュプロー

ブMAC法陰性，INNO-LiPA法ではMAISのみにバンドに発色があり，シークエンス解析で*M. paraffinicum*と判定されたが同時に*M. scrofulaceum* DSM 43992と98.9%の相同性があったと報告している[13]。今回アキュプローブMAC法でMAC，コバス アンプリコア マイコバクテリウム法により*M. avium*と同定された菌株はすべてINNO-LiPA法で明確にMAVに発色が見られ，アキュプローブMAC法でMAC，コバス アンプリコア マイコバクテリウム法により*M. intracellulare*と判定された菌株も上記の菌株23以外はMIN-1に発色が見られた。したがって唯一MIN-2にバンドを示した菌株18は*M. intracellulare* sqv. Mac-Aとかなり相同性が高い近縁菌種と考えられた。

菌株13は16S rRNAシークエンス解析で*M.mucogenicum* ATCC 49650Tと5bpの違い（98.8%の相同性）が見られ*M. mucogenicum*の近縁種と推定された。小川培地上で迅速に発育しDDH法で同定不能，INNO-LiPA法で*M. fortuitum*と判定されており，結果に乖離が見られた。*M. mucogenicum*は古くは*M.chelonae*-likeとして知られていたが，16S rRNA遺伝子では*M. chelonae*よりも*M. fortuitum*に近い系統に位置しており[15]，現在では*M. chelonae-abscessus*グループと*M. fortuitum*グループに近縁の迅速発育菌として独立したグループと定義されている。Ballardらは同じくATCC 49650Tと5 bp違いでなおかつATCC 49649と1bp違いの*M. mucogenicum* N248を解析しており，新しいsubspeciesの可能性があると報告している[16]。迅速発育菌は多様性に富んでおり，菌株13も*M. mucogenicum*のvariant typeの可能性が考えられた。

同じく迅速発育菌であった菌株5はINNO-LiPA法ではMYC genusのみ発色が見られ，DDH法で*M. fortuitum*，シークエンス解析で*M. fortuitum* DSM46621とDSM44220に100%の相同性が認められた。Padillaらは INNO-LiPA法で同じタイプのDSM46621株は*M. fortuitum*と同定されたと報告している[12]。われわれの検討では同菌種のDSM44220株（*M. fortuitum subspecies acetamidolyticum*）はDDH法とINNO-LiPA法で*M. fortuitum*と同定できた（データ未掲載）。*M. fortuitum*はITSシークエンス解析でsqv. Ⅰ～Ⅳが認められており高い多型性を示すため[17]，迅速発育菌の詳細な亜型解析にはシークエンス解析が重要であると思われた。

遺伝子を用いた同定キットによる判定と併行して従来法やコロニー性状から菌種を鑑別することは非常に重要である。菌株22はコバス アンプリコア マイコバクテリウム法，アキュプローブ法，DDH法で同定不能となった遅発育菌である。INNO-LiPA法ではMYC genusの反応が見られたが，シークエンス解析では*M. interjectum*と判定された。*M. interjectum*は非光発色性の遅発育菌でかつ16S rDNA配列が特異的であり，遺伝子を用いた同定キットによる菌種同定は困難である[18]。INNO-LiPA法においても該当プローブが固相化されていないため同菌種の同定はできず，培養でのコロニー性状の観察や生化学的性状試験が鑑別上重要になってくる。同様に菌株2と19は，3種類のプローブで*M. kansasii*の亜型を判別可能であるINNO-LiPA法でMKA-3に発色した。16S rRNA遺伝子のシークエンス解析から*M. kansasii* sqv. ⅢとⅥとに判定されたが研究用試薬アキュプローブ カンサシで陰性となるため*M. kansasii*と判定されなかった。日常検査では光発色試験に及んでいなかったが，改めて実施した結果*M. kansasii*と同定できた。

コロニーの光発色試験での光発色菌，暗発色菌，非光発色菌の鑑別は純培養を用いるため可変的，主観的であり，熟練を要する。*M. szulgai*は37℃で暗発色性，25℃培養で光発色性になる。*M. simiae*の光発色性の出現は通常1時間の光照射のところ6～24時間の光照射が必要であり注意を要する。培養時のコロニー性状の観察において，S型，R型，その移行型（SR型，RS型）の性状が継代を重ねることで変化してくることがある。また発育速度の観察は，遅発育菌でも大量の菌を接種すれば7日ぐらいで発育は見られる場合はあるし，迅速発育菌での分離培養の時にはコロニーの発生までに時間がかかる場合もある。したがって培養条件により変化する菌の性状を十分考慮して，なるべく初代分離菌について詳細に観察することが望ましい。

INNO-LiPA法の製造元であるINNOGENETICS社の本社がベルギーに位置するため，欧米のAIDS患者から分離された*M. genavense*[19]や，イギリス，スコットランド，ウェールズ，スウェーデン，フランスで分離が増えている*M. malmoense*[20]といった菌種に対する同定が可能となっている。わが国では現時点でのこれらの菌種による感染症の報告は非常にまれであるため，今後これら稀少菌種の同定の際には大きな威力を発揮すると思われる。一方，最近わが国で分離の報告が増加している遅発育菌の*M. lentiflavum*[14]が今回シークエンス解析により9株確認されたが，対応プローブが配置されていないINNO-LiPA法ではMYC genusにしかバンドの発色が見られず同定に至らなかった。臨床での有用性をより高めるために，わが国の抗酸菌分離状況にあわせたINNO-LiPA法の仕様改良を切望したい。

今回有用性が認められたINNO-LiPA法は手技面でもPCR増幅後約3時間で判定可能であり，迅速性が証明された。ハイブリダイゼーションから洗浄，発色までを行う自動化ハイブリダイゼーション装置Auto-LiPAを利用すれば労力の軽減が可能であると思われる。またINNO-LiPA法はストリップ上に得られるバンドの有無で判定するため，DDH法のような読み取り時の測定誤差は少

なくなると考えられる。複数菌混合培養における複数菌種同定も可能であることから，単一分離培養に要する時間や手間が省かれ，迅速に同定結果が得られることが明らかとなった。

抗酸菌における遺伝子検査の進歩は特に目覚ましく，今回用いた検査法も含めて多様な検査キットが市販されている。各種キットの特徴を熟知したうえでそれぞれの施設に適した検査法を選択し，各キット間に生じる結果の乖離や同定不能な株が存在する場合を考慮して菌種同定を行うことが望まれる。またこれらキットは定性用検査であり，検体内の菌量を反映できないため，塗抹・培養検査の結果と同定結果とを鑑みて治療方針を決定することが重要である。特にNTMを分離した場合には非結核性抗酸菌症の診断基準[21)22)]と合わせて総合的に判断するべきである。

文　献

1) Ichiyama S, Iinuma Y, Tawada Y, et al.: Evaluation of Gen-Probe Amplified Mycobacterium Tuberculosis Direct Test and Roche PCR-microwell plate hybridization method (AMPLICOR MYCOBACTERIUM) for direct detection of mycobacteria. J Clin Microbiol. 1996 ; 34 : 130−133.
2) Abe C, Hirano K, Wada M, et al.: Detection of *Mycobacterium tuberculosis* in clinical specimens by polymerase chain reaction and Gen-Probe Amplified Mycobacterium Tuberculosis Direct Test. J Clin Microbiol. 1993 ; 31 : 3270−3274.
3) Wobeser WL, Krajden M, Conly J, et al.: Evaluation of Roche Amplicor PCR assay for *Mycobacterium tuberculosis*. J Clin Microbiol. 1996 ; 34 : 134−139.
4) 前倉亮治，横田総一郎，小倉　剛：抗酸菌感染症診断の進歩．分子呼吸病．1998 ; 2 : 346−352.
5) Lebrun L, Espinasse F, Poveda JD, et al.: Evaluation of nonradioactive DNA probes for identification of mycobacteria. J Clin Microbiol. 1992 ; 30 : 2476−2478.
6) Reisner BS, Gatson AM, Woods GL: Use of Gen-Probe AccuProbes to identify *Mycobacterium avium* complex, *Mycobacterium tuberculosis* complex, *Mycobacterium kansasii*, and *Mycobacterium gordonae* directly from BACTEC TB broth cultures. J Clin Microbiol. 1994 ; 32 : 2995−2998.
7) Kusunoki S, Ezaki T, Tamesada M, et al.: Application of colorimetric microdilution plate hybridization for rapid genetic identification of 22 *Mycobacterium* species. J Clin Microbiol. 1991 ; 29 : 1596−1603.
8) 山崎利雄，高橋　宏，中村玲子：マイクロプレートハイブリダイゼーション法による抗酸菌同定法の検討．結核．1993 ; 68 : 5−11.
9) 斉藤　宏，長友雅彦，中篤雅信，他：DNA-DNA Hybridizationを原理とする「DDHマイコバクテリア '極東'」を用いた抗酸菌同定とその同定精度の検討．JARMAM. 1994 ; 6 : 23−28.
10) Tortoli E, Mariottini A, Mazzarelli G : Evaluation of INNO-LiPA MYCOBACTERIA v2 : improved reverse hybridization multiple DNA probe assay for mycobacterial identification. J Clin Microbiol. 2003 ; 41 : 4418−4420.
11) Miller N, Infante S, Cleary T: Evaluation of the LiPA MYCOBACTERIA assay for identification of mycobacterial species from BACTEC 12B bottles. J Clin Microbiol. 2000 ; 38 : 1915−1919.
12) Padilla E, González V, Manterola JM, et al.: Comparative evaluation of the new version of the INNO-LiPA Mycobacteria and GenoType Mycobacterium assays for identification of *Mycobacterium* species from MB/BacT liquid cultures artificially inoculated with mycobacterial strains. J Clin Microbiol. 2004 ; 42 : 3083−3088.
13) Lebrun L, Weill FX, Lafendi L, et al.: Use of the INNO-LiPA-MYCOBACTERIA assay (version 2) for identification of *Mycobacterium avium−Mycobacterium intracellulare−Mycobacterium scrofulaceum* complex isolates. J Clin Microbiol. 2005 ; 43 : 2567−2574.
14) 岩本朋忠，中永和枝，石井則久，他：*Mycobacterium lentiflavum*の菌種内塩基配列変異に関する研究．結核．2008 ; 83 : 417−422.
15) Springer B, Böttger EC, Kirschner P, et al.: Phylogeny of the *Mycobacterium chelonae*-like organism based on partial sequencing of the 16S rRNA gene and proposal of *Mycobacterium mucogenicum* sp. nov. Int J Syst Bacteriol. 1995 ; 45 : 262−267.
16) Ballard J, Turenne CY, Wolfe JN, et al.: Molecular characterization of nontuberculous mycobacteria isolated from human cases of disseminated disease in the USA, Thailand, Malawi, and Tanzania. J Gen Appl Microbiol. 2007 ; 53 : 153−157.
17) Richter E, Niemann S, Rüsch-Gerdes S, et al.: Identification of *Mycobacterium kansasii* by using a DNA probe (Accu Probe) and molecular techniques. J Clin Microbiol. 1999 ; 37 : 964−970.
18) Tortoli E: Impact of genotypic studies on mycobacterial taxonomy: the new mycobacteria of the 1990s. Clin Microbiol Rev. 2003 ; 16 : 319−354.
19) Bogdan C, Kern P, Richter E, et al.: Systemic infection with *Mycobacterium genavense* following immunosuppressive therapy in a patient who was seronegative for human immunodeficiency virus. Clin Infect Dis. 1997 ; 24 : 1245−1247.
20) The Research Committee of the British Thoracic Society: Pulmonary disease caused by *M. malmoense* in HIV negative patients: 5-yr follow-up of patients receiving standardised treatment. Eur Respir J. 2003 ; 21 : 478−482.
21) Griffith DE, Aksamit T, Brown-Elliott BA, et al., on behalf of the ATS Mycobacterial Diseases Subcommittee : An Official ATS/IDSA Statement: Diagnosis, Treatment, and Prevention of Nontuberculous Mycobacterial Diseases. Am J Respir Crit Care Med. 2007 ; 175 : 367−416.
22) 日本結核病学会非結核性抗酸菌症対策委員会，日本呼吸器学会感染症・結核学術部会：肺非結核性抗酸菌症診断に関する指針—2008年．結核．2008 ; 83 : 525−526.

Original Article

EVALUATION OF THE INNO-LiPA MYCOBACTERIA v2 FOR MYCOBACTERIAL IDENTIFICATION

[1]Shiomi YOSHIDA, [1]Katsuhiro SUZUKI, [1]Kazunari TSUYUGUCHI, [4]Tomotada IWAMOTO, [2]Motohisa TOMITA, [1]Masaji OKADA, and [3]Mitsunori SAKATANI

Abstract [Purpose] Evaluation of the INNO-LiPA MYCOBACTERIA v2 (the INNO-LiPA assay) for mycobacterial identification.

[Materials and Methods] The laboratory identifications consisting of Cobas Amplicor systems, AccuProbe, and DDH, are commonly used to identify mycobacterial isolates in Japan. We compared the results between the INNO-LiPA assay and the common methods. A total of 122 clinical isolates from NHO Kinki-chuo Chest Medical Center from 1 February to 30 June 2006 were tested.

[Results] There was agreement between the INNO-LiPA assay and the common methods for 112 mycobacterium isolates. The six discordant isolates have showed same results between sequencings and the INNO-LiPA assay. The one *M. fortuitum* isolates was indicated correctness by DDH and the one *M. intracellulare* isolates was recognized by Cobas Amplicor systems and as MAC by AccuProbe MAC. Moreover, discrepant results between sequencings and mycobacterial identifications including the INNO-LiPA assay were 2 isolates (*M. paraffinicum*, *M. mucogenicum* variant type).

[Conclusion] The INNO-LiPA assay could provide rapid and correct identification results with clear-cut and easy interpretation.

Key words: Mycobacteria, INNO-LiPA MYCOBACTERIA v2, Identification, 16S rRNA gene, ITS sequencing

[1]Clinical Research Center, [2]Department of Clinical Laboratory, [3]Department of Respiratory Medicine, National Hospital Organization (NHO) Kinki-chuo Chest Medical Center, [4]Kobe Institute of Health

Correspondence to: Shiomi Yoshida: Clinical Research Center, NHO Kinki-chuo Chest Medical Center, 1180 Nagasone-cho, Kita-ku, Sakai-shi, Osaka 591−8555 Japan. (E-mail: dustin@kch.hosp.go.jp)

Journal of Medical Microbiology (2008), 57, 873–880 DOI 10.1099/jmm.0.47564-0

Promising loci of variable numbers of tandem repeats for typing Beijing family *Mycobacterium tuberculosis*

Yoshiro Murase, Satoshi Mitarai, Isamu Sugawara, Seiya Kato and Shinji Maeda

Correspondence
Shinji Maeda
maeda@jata.or.jp

Research Institute of Tuberculosis, Japan Anti-Tuberculosis Association, 3-1-24 Matsuyama, Kiyose, Tokyo 204-8533, Japan

We analysed the genotypes of 325 *Mycobacterium tuberculosis* clinical isolates obtained during 2002 throughout Japan. The genotyping methods included insertion sequence IS*6110* RFLP, spoligotyping and variable number of tandem repeat (VNTR) analyses. Clustered isolates revealed by IS*6110* RFLP analysis accounted for 18.5% (60/325) of the isolates. Beijing genotype tuberculosis (TB) accounted for 73.8% (240/325) of the isolates. Using VNTR, we analysed 35 loci, including 12 standard mycobacterial interspersed repetitive units and 4 exact tandem repeats. The discriminatory power of these 16 loci was low. Using VNTR analyses of the 35 loci, 12 loci (VNTRs 0424, 0960, 1955, 2074, 2163b, 2372, 2996, 3155, 3192, 3336, 4052 and 4156) were selected for the genotyping of Beijing genotype strains. Comparison of the discriminatory power of the 12-locus VNTR [Japan Anti-Tuberculosis Association (JATA)] to that of the 15-locus and 24-locus VNTRs proposed by Supply *et al.* (2006) showed that our established VNTR system was superior to the reported 15-locus VNTR and had almost equal discriminatory power to the 24-locus VNTR. This 12-locus VNTR (JATA) can therefore be used for TB genotyping in areas where Beijing family strains are dominant.

Received 8 August 2007
Accepted 13 March 2008

INTRODUCTION

RFLP analysis using insertion sequence IS*6110* is the gold standard of tuberculosis (TB) genotyping (Cave *et al.*, 1991; Kremer *et al.*, 1999; van Embden *et al.*, 1993). However, this RFLP analysis has many associated problems (Mostrom *et al.*, 2002).

Spoligotyping has been used throughout the world as a convenient and reproducible PCR-based method for genotyping (Kamerbeek *et al.*, 1997). Nevertheless, it provides little information related to Beijing family strains because spoligotypes of this genotype family show very little variation (Glynn *et al.*, 2002; Kremer *et al.*, 2004). In the countries of eastern Asia, the frequency of Beijing genotype TB is high. For that reason, spoligotyping is ineffective to discriminate unrelated isolates.

Analysis of variable number of tandem repeat (VNTR) loci is a promising PCR-based typing method. In VNTR analysis, some mini-satellite loci in the *Mycobacterium tuberculosis* genome are amplified using PCR; then their copy numbers are determined (Smittipat & Palittapongarnpim, 2000; Supply *et al.*, 2000). In fact, VNTR analysis with the standard 12 loci of mycobacterial interspersed repetitive units (MIRUs) has been used in the USA and Europe (Blackwood *et al.*, 2004; Mazars *et al.*, 2001). The Centers for Disease Control and Prevention (CDC) in the USA have adopted the standard 12-locus MIRU-VNTR for TB analyses (Cowan *et al.*, 2005; CDC, 2004). However, the discriminatory power of 12-locus MIRU-VNTR has been found to be insufficient (Supply *et al.*, 2006), which similarly applies to Beijing genotype TB analyses (Kam *et al.*, 2005; Kremer *et al.*, 2005; Nikolayevskyy *et al.*, 2006). Several reports have described other loci. Almost all corresponding loci have been described in the relevant literature (Iwamoto *et al.*, 2007; Kam *et al.*, 2006; Wada *et al.*, 2007).

It is noteworthy that a new 15-locus or 24-locus MIRU-VNTR method has been proposed in Europe (Oelemann *et al.*, 2007; Supply *et al.*, 2006). These new VNTR loci have had a distinct impact on genotyping of the Beijing family, but some large clusters remain (Iwamoto *et al.*, 2007). Therefore, several VNTR loci must be added to the reported 15-locus VNTR method for analyses of Beijing genotype strains (Yokoyama *et al.*, 2007).

For exploring the diversity of VNTR loci, we performed genotyping of IS*6110* RFLP, spoligotyping and 35-locus VNTR analysis using TB isolates from all over Japan. Based

Abbreviations: CDC, Centers for Disease Control and Prevention; ETR, exact tandem repeat; HGDI, Hunter–Gaston discriminatory index; JATA, Japan Anti-Tuberculosis Association; MIRU, mycobacterial interspersed repetitive unit; TB, tuberculosis; VNTR, variable number of tandem repeats.

on these results, we propose a VNTR system that has the same discriminatory power as RFLP for analysis of a minimum number of loci in countries where the Beijing family has spread. Moreover, the results provide useful information for molecular epidemiological analyses of TB in regions where the Beijing genotype is dominant.

METHODS

***M. tuberculosis* isolates.** In all, 325 *M. tuberculosis* isolates, 3–10 strains per prefecture, were selected randomly from among 3122 isolates collected for a drug-resistance survey conducted in Japan in 2002 by the Tuberculosis Research Committee (RYOKEN). The isolates that we analysed had been originally considered as low cluster because the possibility of contact among patients was quite low. For comparing results of RFLP and VNTR analyses, 76 *M. tuberculosis* isolates were collected from 25 suspected epidemic outbreaks, along with epidemiological information. The epidemiologically linked 17 clusters (54 strains) showed the same RFLP pattern in each case. The 8 initially suspected TB patient clusters (22 strains) were found to be independent simultaneous occurrences: each strain had a different RFLP pattern. Mycobacterial genomic DNA was prepared from bacteria grown on Ogawa medium using an Isoplant kit (Nippon Gene).

Molecular typing methods. For this study, IS*6110* RFLP typing was performed according to a standardized protocol (van Embden *et al.*, 1993); band patterns were analysed using the BioNumerics software package (Applied Maths). In RFLP analysis, strains that have an identical band pattern were categorized as a cluster. Spoligotyping was also performed according to a standard protocol (Kamerbeek *et al.*, 1997). Sequences of primers used for amplification of 12 MIRU loci (MIRU-02, 04, 10, 16, 20, 23, 24, 26, 27, 31, 39 and 40), 4 exact tandem repeats (ETRs) (ETR-A, B, C and F) and 19 other loci (VNTRs 0424, 1612, 1895, 1955, 2074, 2163a, 2163b, 2347, 2372, 2401, 3155, 3171, 3232, 3336, 3690, 3820, 4052, 4120 and 4156) for VNTR were selected (Frothingham & Meeker-O'Connell, 1998; Iwamoto *et al.*, 2007; Roring *et al.*, 2002; Smittipat *et al.*, 2005; Supply *et al.*, 2001, 2006). The VNTR typing was performed using Ex *Taq* with GC PCR buffer I (Takara Bio). The PCR mixture was prepared in a 20 µl volume with 1 × GC PCR buffer I, 0.5 U Ex *Taq*, 200 µM each of four dNTPs, 0.5 µM each of the primer set and 10 ng template DNA. Then PCR was carried out for all loci under the following conditions: initial denaturation at 94 °C for 5 min, and then 35 cycles of 94 °C for 30 s, 63 °C for 30 s and 72 °C for 3 min, followed by a final extension at 72 °C for 7 min.

Estimation of molecular size of amplified DNA fragments. The sizes of the amplified DNA fragments were determined using a capillary array electrophoresis analysis system (*i*-Chip SV1210; Hitachi Electronics Engineering) (Sonehara *et al.*, 2006) or an ABI 3130 genetic analyser (Applied Biosystems) with the GeneMapper program (Applied Biosystems). The *i*-Chip was used to calibrate VNTR analysis and the genetic analyser was used to analyse the standard 12 loci MIRU (Iwamoto *et al.*, 2007; Supply *et al.*, 2001). Alternatively, the PCR products were analysed in a 2–2.5 % agarose gel. Their respective copy numbers were calculated from their size and assigned according to the number of repeats for each locus (Frothingham & Meeker-O'Connell, 1998; Kremer *et al.*, 2005; Skuce *et al.*, 2002; Supply *et al.*, 2001). The calculation accuracy was confirmed through analysis of *M. tuberculosis* H37Rv.

Allelic diversity and discrimination. The allelic diversity (h) at each VNTR locus was calculated using the index $h=1-\Sigma x_i^2$, where x_i is the frequency of the ith allele at the locus, as used in other studies (Kremer *et al.*, 2005; Sun *et al.*, 2004). The Hunter–Gaston discriminatory index (HGDI) was calculated in accordance with a method explained in another paper (Hunter & Gaston, 1988) to evaluate the combination of some VNTR loci.

Combinations of VNTR loci. For the following combination of VNTR loci, the HGDI were compared: 15-locus VNTR [Supply (15)] – VNTRs 0424, 0577, 0580, 0802, 0960, 1644, 1955, 2163b, 2165, 2401, 2996, 3192, 3690, 4052 and 4156; 24-locus VNTR [Supply (24)] – Supply (15) + VNTRs 0154, 2059, 2347, 2461, 2531, 2687, 3007, 3171 and 4348; 12-locus VNTR [Japan Anti-Tuberculosis Association (JATA) (12)] – VNTRs 0424, 0960, 1955, 2074, 2163b, 2372, 2996, 3155, 3192, 3336, 4052 and 4156.

RESULTS AND DISCUSSION

RFLP, spoligotyping and MIRU-VNTR analyses in Japan

From throughout Japan, 325 collected isolates were analysed using IS*6110* RFLP (Table 1). The percentage of clustered isolates was 18.5 % (60/325). In spoligotyping, 293 (90 %) isolates formed clusters; the maximum cluster size was 228. The largest cluster was composed of the Beijing genotype [70.2 % (228/325)]. Because the number of Beijing-like strains was 12 (Kremer *et al.*, 2004), the total of Beijing genotype strains used in this experiment was 240 (73.8 %). The Beijing family strains were confirmed to be dominant in Japan. The CDC in the USA has adopted the standard 12-locus MIRU-VNTR for TB analyses (Cowan *et al.*, 2005; CDC, 2004). We analysed the 325 TB isolates using 12-locus MIRU-VNTR and 16-locus VNTR (12 standard MIRU and 4 ETRs). There were only 89 unique types in the 12-locus MIRU-VNTR. The percentage of clustered isolates decreased from 72.6 % (12-MIRU-VNTR) to 62.8 % (16-locus VNTR) when the ETR loci were added to 12-locus MIRU analysis. Both rates of clustered isolates in VNTR analysis were higher than in RFLP (18.5 %). Furthermore, the HGDI showed that the discriminatory power of IS*6110* RFLP was the highest of all analyses used for this study: spoligotyping, 12-locus MIRU-VNTR and 16-locus VNTR.

An optimal 15-locus VNTR has been proposed by a consortium of European and American laboratories as a new worldwide standard method for discriminating TB genotypes using 52 different groups of related strains from different countries (Supply *et al.*, 2006). This VNTR method can discriminate in greater detail than the standard 12-locus MIRU-VNTR when the Beijing genotype of TB is analysed. However, it has been reported that the discriminatory power of 15-locus VNTR is insufficient for analysis of the Beijing genotype (Iwamoto *et al.*, 2007). The frequency of the Beijing family in Japan (80 % of total TB) (Yokoyama *et al.*, 2007) differs greatly from that in the USA (16 %) and European countries (4 %) (Filliol *et al.*, 2002). For that reason, new loci are necessary to analyse the Beijing family more effectively in Japan, Korea, China and other Asian countries.

Table 1. Comparison of the discriminatory power of IS*6110* RFLP, spoligotyping and VNTR analyses

Typing method	Total no. of type patterns	No. of unique types	No. of clusters	No. of clustered isolates (%)	Maximum no. of isolates in a cluster	HGDI*
IS*6110* RFLP	283	265	18	60 (18.5)	8	0.998
Spoligotyping	45	32	13	293 (90.2)	228	0.501
12-locus MIRU-VNTR	127	89	38	236 (72.6)	61	0.944
16-locus VNTR (12 MIRU and 4 ETRs)	165	121	44	204 (62.8)	44	0.967
8-locus VNTR (VNTRs 2163b, 4052, 3336, 1955, 4156, 2372, 0424 and 2074)	290	265	25	60 (18.5)	5	0.999
10-locus VNTR (8-locus VNTR + VNTRs 2996 and 3155)	297	276	21	49 (15.1)	4	0.999
12-locus VNTR (JATA) (10-locus VNTR + VNTRs 0960 and 3192)	302	284	18	41 (12.6)	4	0.999
15-locus VNTR (Supply)	291	269	22	56 (17.2)	6	0.999
24-locus VNTR (Supply)	303	287	16	38 (11.7)	4	0.999

*HGDI was calculated as described in Methods.

VNTR analyses of 19 loci

Different loci from those used for the USA or European countries must be examined when VNTR analysis is adopted for TB genotyping in Japan. Actually, VNTR analyses of 48 loci using 21 Beijing isolates have been reported (Smittipat *et al.*, 2005). Some loci that had high *h* for Beijing genotyping strains and other loci, such as Queen's University Belfast (QUB), were selected (Skuce *et al.*, 2002). In fact, 19 loci of 325 TB isolates were analysed using VNTR (Table 2). It was generally difficult to obtain the exact copy number using agarose gel electrophoresis in VNTR analysis when the molecular size of the PCR product was greater than 1 kb. More than 15 copies of repetitive units (larger than 1 kb) were detected at VNTRs 2163a, 2163b, 1895, 3232, 3336, 3820 and 4120. Only a few isolates had more than 15 copies of repetitive units at the loci of VNTRs 2163b, 1895 and 3336. However, for analyses of VNTRs 2163a, 3232, 3820 and 4120, more than 4 % of total isolates (18, 86, 50 and 14 strains, respectively) had 15 or more copies. For that reason, it was difficult to interpret the exact copy number. Furthermore, multiple PCR products were detected at the respective loci of VNTRs 2163b, 3232, 3336, 3820, 4120 and 4156. These had the potential to be unstable loci in VNTR analysis, and might be in the process of copy number change. Moreover, no PCR product was found in analyses of VNTRs 2163a, 2163b, 4052, 0424 and 2347.

From Japan, it was reported that VNTRs 3232, 3820 and 4120 are the hyper-variable loci (Iwamoto *et al.*, 2007; Wada *et al.*, 2007; Yokoyama *et al.*, 2007). More than 5 % of total isolates presented analytical problems (absence of PCR product, PCR products difficult to interpret or amplification of multiple alleles) at the loci of VNTRs 2163a, 3232, 3820 and 4120. Therefore, to obtain stable and precise VNTR results, these four loci were excluded from VNTR analyses of Beijing family strains.

New combination of VNTR loci for TB typing in Japan

The discriminatory power of each locus, based on the *h* values of all isolates, is presented in Table 3. The *h* of non-Beijing family strains was higher than that of the Beijing strain, except for VNTRs 0424, 2163b and 4156. These three loci were indispensable for distinction of the Beijing family.

One purpose of this study is to establish a new VNTR system with equal discriminatory power to that of RFLP using a minimum loci analysis in countries where the Beijing family is prevalent. Combinations of some loci, such as the top 8 loci (8-locus VNTR), top 10 loci (10-locus VNTR) or top 12 loci (12-locus VNTR), were compared to those of IS*6110* RFLP (Table 1) in terms of several characteristics, such as the number of unique isolates and clusters. In fact 8-locus VNTR had resolution performance that was equal to IS*6110* RFLP analysis in terms of the number of independent isolates and the rate of clustered isolates. Therefore, the 10-locus and 12-locus VNTRs were superior to IS*6110* RFLP. However, the quantities of clusters in VNTR analysis were comparable to those of RFLP only when 12-locus VNTR was used. Consequently, the primer set of the 12-locus VNTR (JATA) was ultimately selected for VNTR analysis in Japan.

Comparison of the discriminatory power of IS*6110* RFLP and VNTR analyses

A novel standard, optimized 15-locus and 24-locus VNTR primer sets (Supply *et al.*, 2006), was proposed recently (Table 3). The respective discriminatory powers of IS*6110* RFLP and VNTRs [15-locus (Supply) (Supply *et al.*, 2006), 24-locus (Supply) and 12-locus (JATA)] were compared using the percentage of clustered isolates (Fig. 1). The fraction of clustered isolates of 12-locus VNTR (JATA)

Table 2. The allelic profiles of 19 additional VNTR loci in 325 *M. tuberculosis* strains

VNTR locus	No. amplification	Multiple PCR products	Copy no. of repetitive unit(s)														
			0	1	2	3	4	5	6	7	8	9	10	11	12	13	14	15 and over*
2163a (QUB-11a)	5				10	27	5	12	27	10	30	103	51	15	5		7	18
2163b (QUB-11b)	3	1		6	29	56	35	35	35	75	39	6	1	2	1			1
3155 (QUB-15)					8	29	62	199	24	3								
1612 (QUB-23)							1		2	321	1							
4052 (QUB-26)	1		2	8	36	6	15	23	27	58	114	18	11	5	1			2
1895				3	40	14	255	3	4		4							
1955			4	29	41	141	71	31	2		1	1	3	1				
2074				18	83	179	39	6										
2372			1	22	78	156	58	7	3									
2401				6	114	4	200	1										
3232		1	1	8		2	23	25	5	8	6	17	18	27	36	22	40	86
3336		1	3	13	8	20	138	59	20	16	7	17	9	7	2	2	1	2
3820		1		2	9	10	32	9	6	9	12	14	8	31	51	44	37	50
4120		3	1	19	26	25	27	11	19	21	28	29	44	21	19	9	9	14
4156		1		12	96	75	131	10										
0424	1			15	72	61	171	4	1									
2347	1				13	8	302		1									
3171				1	2	319		3										
3690				6	17	248	19	21	7	7								

*The number of strains that had more than 15 copies in the locus are represented together in this column.

Table 3. The *h* values for each locus and details of the VNTR loci selected for the different VNTR analyses

No.	Locus	Alias	*h**			This study	Supply *et al.* (2006)†		12 MIRU +4 ETRs
			All isolates (n=325)	Beijing family (n=240)	Non-Beijing (n=85)	12 VNTR	24 VNTR	15 VNTR	
1	2163b	QUB 11b	0.855	0.815	0.802	×	×	×	
2	4052	QUB 26	0.812	0.764	0.860	×	×	×	
3	3336	VNTR 3336	0.768	0.642	0.894	×			
4	1955	Mtub 21	0.731	0.598	0.696	×	×	×	
5	4156	VNTR 4156	0.693	0.623	0.564	×	×	×	
6	2372	VNTR 2372	0.675	0.595	0.672	×			
7	0424	Mtub 04	0.635	0.468	0.425	×	×	×	
8	2074	Mtub 24	0.614	0.591	0.615	×			
9	2996	MIRU 26	0.591	0.314	0.667	×	×	×	×
10	3155	QUB 15	0.575	0.537	0.639	×			
11	0960	MIRU 10	0.546	0.431	0.704	×	×	×	×
12	3192	MIRU 31	0.545	0.270	0.416	×	×	×	×
13	2401	Mtub 30	0.498	0.379	0.463		×	×	
14	2165	ETR A	0.496	0.223	0.446		×	×	×
15	0802	MIRU 40	0.473	0.229	0.697		×	×	×
16	4348	MIRU 39	0.472	0.156	0.543		×		×
17	3690	Mtub 39	0.406	0.215	0.745		×	×	
18	1895	VNTR 1895	0.367	0.337	0.447				
19	3239	ETR F	0.358	0.237	0.575				×
20	1644	MIRU 16	0.345	0.258	0.502		×	×	×
21	2531	MIRU 23	0.336	0.158	0.555		×		×
22	0580	MIRU 4	0.189	0.049	0.484		×	×	×
23	2461	ETR B	0.151	0.017	0.447		×		×
24	0577	ETR C	0.134	0.057	0.317		×	×	×
25	2347	Mtub 29	0.129	0.095	0.214		×		
26	2059	MIRU 20	0.083	0.065	0.131		×		×
27	3007	MIRU 27	0.072	0.081	0.046		×		×
28	2687	MIRU 24	0.054	0	0.193		×		×
29	3171	Mtub 34	0.036	0.033	0.046		×		
30	1612	QUB 23	0.024	0.025	0.023				
31	0154	MIRU 2	0.018	0.008	0.046		×		×
32 (excluded)	3232	VNTR 3232	0.929	0.909	0.834				
33 (excluded)	4120	VNTR 4120	0.924	0.902	0.767				
34 (excluded)	3820	VNTR 3820	0.911	0.871	0.824				
35 (excluded)	2163a	QUB 11a	0.836	0.752	0.858				

*h represents the allelic diversity of each locus, calculated as described in Methods.
†The combination of 15- and 24-locus VNTR analyses were reported by Supply *et al.* (2006).

(12.6%) was superior to that of RFLP (18.5%) and 15-locus VNTR (Supply) (17.2%) in this experiment. The respective discriminatory capabilities of 15-locus and 24-locus VNTR (Supply) and 12-locus VNTR (JATA) were better than that of IS*6110* RFLP.

Our newly established 12-locus VNTR (JATA) typing method had almost equivalent discriminatory power to that of 24-locus VNTR (Supply) for TB genotyping, although it uses only 12 loci. In the 12-locus VNTR (JATA), 8 loci overlap with the 15-locus and 24-locus VNTRs (Supply): 4 loci (VNTRs 2074, 2372, 3155 and 3336) are independent. In the Supply VNTR typing method (Supply *et al.*, 2006), VNTR 3336 was discarded from the final selection for detection because of the following observations: it gave multiple PCR products, it did not give a PCR product and there was a lack of reproducibility between results obtained in independent laboratories. 'No PCR amplification' represents a characteristic typing datum; it indicates that the strain has different sequences in the primer binding site or has no such region. In addition, detection of a multiple PCR product might signify that a conversion of copy number is occurring at the locus, meaning that the genetic stability of such loci is not high.

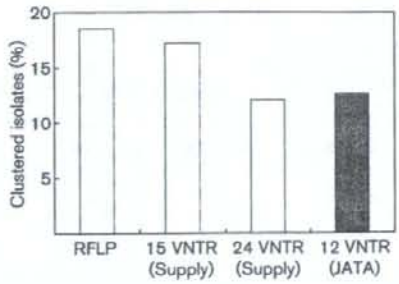

Fig. 1. Comparison of clustering rates in RFLP and VNTR analyses. The percentage of clustered isolates was calculated for each case.

Our data showed that the *h* of VNTR 3336 gave a maximum value in non-Beijing TB analysis (Table 3). The genetic clock of VNTR 3336 in non-Beijing genotypes might be faster than that of Beijing strains. Therefore, the locus of VNTR 3336 in non-Beijing strains might be unstable and that in Beijing strains might be stable. Consequently, the locus of VNTR 3336 might be used in 12-locus VNTR (JATA).

In this study, 325 independent isolates (with no epidemiological link) were collected and analysed. Results show that only four strains formed clusters in both the RFLP (60 strains) and VNTR (41 strains) methods: RKN 246, RKN 275, RKN 283 and RKN 319. The remaining clusters were subdivided using the other method. Cluster 08 of RFLP analysis comprised six strains including the four clustered strains. By 12-locus (JATA) VNTR, cluster 08 was further divided into three groups (Fig. 2). The two remaining strains (RKN 177 and RKN 215) showed independent patterns. Differences of copy number in the two strains were found in two loci. The respective discriminatory powers of RFLP and VNTR analyses were different. The maximum cluster sizes in IS*6110* RFLP and JATA (12) VNTR were, respectively, 8 and 4 (data not shown). The 12-locus (JATA) VNTR had a higher discrimination power than RFLP analysis did.

Analysis of clinical isolates from a suspected outbreak using 12-locus VNTR (JATA)

For examining the effectiveness of the 12-locus VNTR (JATA), 25 clusters (76 strains in total) were analysed. Of them, 17 clusters (54 strains) for which the RFLP patterns were identical in each group had the same VNTR profile (data not shown). Eight initially suspected TB patient clusters (22 strains) were not outbreak related (concurrence of TB): their IS*6110* RFLP showed different patterns. These strains are clearly independent. Therefore, the VNTR profile was also expected to show variant patterns in the respective groups. The VNTR analyses using 12-locus VNTR (JATA) showed that each strain had a different profile in at least 5 loci, except for case 6. Analyses of the other isolates also revealed that the discriminatory power of 12-locus VNTR (JATA) was roughly equivalent to that of IS*6110* RFLP analysis.

In case six, strains S-054 and S-160 differed by only one locus (VNTR 2074). Their RFLP patterns were notably different (data not shown). This concomitant change in two independent markers suggests that these two isolates originated from independent clones. They could still very well represent an outbreak if strains were to have highly similar RFLP (differing by only one or two bands) and have identical VNTR profiles. It is impossible to determine whether or not this was a mass infection case. For that reason, a conclusion should be offered only after considering all results, including contact examination and epidemiological investigation.

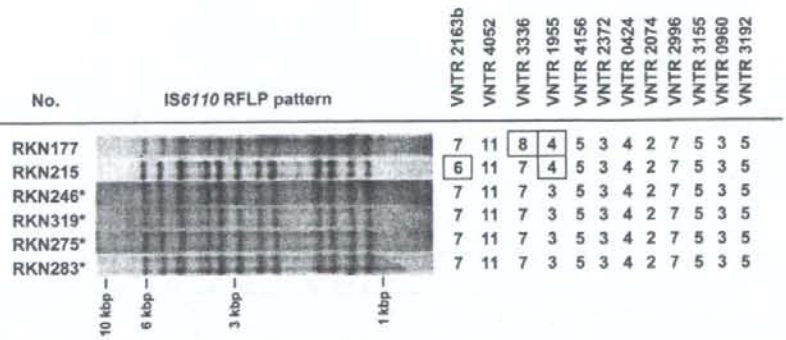

Fig. 2. The subdivision of cluster 08 in IS*6110* RFLP using 12-locus (JATA) VNTR. Cluster 08 in RFLP analysis comprised six strains. The JATA-VNTR divided cluster 08 into three groups. The isolates marked with an asterisk (RKN246, RKN275, RKN283 and RKN319) were clustered using both RFLP and VNTR analyses. Differences in VNTR patterns are boxed.